Green Chemical Technology

SCIEPublish

Review

Porous Carbon-Based Adsorbents for CO_2 Sequestration from Flue Gases: Tuning Porosity, Surface Chemistry, and Metal Impregnation for Sustainable Capture

Jiaqiang Wang [1], Guohui Yang [2], Ling Wu [3], Binghua Zhou [4], Zhipeng Wang [4], Zhenghong Huang [5], Gang Liu [6] and Mingxi Wang [1,*]

[1] Key Laboratory of Biomass-Based Materials for Environment and Energy in Petroleum & Chemical Industries, School of Chemical and Environmental Engineering, Wuhan Institute of Technology, Wuhan 430205, China; 22409010055@stu.wit.edu.cn (J.W.)

[2] Sichuan Mineral Electromechanic Technician College, Chengdu 610500, China; webmaster@emtc.cn (G.Y.)

[3] Hubei Province Key Laboratory of Coal Conversion and New Carbon Materials, School of Chemistry and Chemical Engineering, Wuhan University of Science and Technology, Wuhan 430081, China; wuling2018@wust.edu.cn (L.W.)

[4] Institute of Advanced Materials, College of Chemistry and Chemical Engineering, Jiangxi Normal University, 99 Ziyang Avenue, Nanchang 330022, China; zhoubh@jxnu.edu.cn (B.Z.); wangzhipeng@jxnu.edu.cn (Z.W.)

[5] Lab of Advanced Materials, School of Materials Science and Engineering, Tsinghua University, Beijing 100084, China; zhhuang@tsinghua.edu.cn (Z.H.)

[6] Hubei Key Laboratory of Plasma Chemistry and Advanced Materials, School of Materials Science and Engineering, Wuhan Institute of Technology, Wuhan 430205, China; gangliu83@wit.edu.cn (G.L.)

* Corresponding author. E-mail: wangmx@wit.edu.cn (M.W.)

Received: 5 December 2025; Revised: 7 January 2026; Accepted: 13 January 2026; Available online: 20 January 2026

ABSTRACT: Escalating atmospheric CO_2 levels and the consequent climate crisis have become urgent imperatives for advancing efficient carbon capture technologies. Porous carbon adsorbents stand out as a leading candidate in this field, owing to their inherently high specific surface areas, tailorable pore architectures, and cost advantages over conventional solid adsorbents. This review focuses on recent progress in the rational engineering of porous carbons for boosted CO_2 capture performance, with a particular emphasis on three complementary modification pathways: pore structure refinement, surface functional group regulation, and metal oxide incorporation. We begin by clarifying the distinct mechanisms of CO_2 physisorption and chemisorption on carbonaceous surfaces, while also elucidating how key operating parameters (temperature, pressure) and real-world flue gas components (e.g., water vapor, SO_2) modulate adsorption behavior. Critical evaluation is then given to strategies for enhancing three core performance metrics—CO_2 uptake capacity, selectivity over N_2, and cyclic stability—including the construction of sub-nanometer micropores (<0.8 nm) for efficient low-pressure CO_2 capture, the introduction of nitrogen- and oxygen-containing moieties to strengthen dipole–quadrupole interactions with CO_2 molecules, and the loading of alkaline metal oxides (e.g., MgO, CaO) to enable reversible chemisorption, which is especially beneficial under humid conditions. Finally, we outline the key challenges that hinder the practical application of porous carbon adsorbents, such as the design of hierarchical pores for both high uptake and fast mass transfer, the precise control of heteroatom doping sites and concentrations, and the mitigation of competitive adsorption in complex multicomponent flue

gases. Corresponding future research priorities are also proposed, with a focus on scalable and sustainable synthesis routes using biomass or waste precursors. Ultimately, this review seeks to provide targeted insights for the rational design of high-performance porous carbon adsorbents, thereby accelerating their deployment in sustainable CO_2 capture systems.

Keywords: CO_2 capture; Porous carbon adsorbents; Porosity tuning; Surface modification; Metal impregnation; Sustainable technology

1. Introduction

The issue of global warming is now widely understood to stem from the persistent release of large quantities of greenhouse gases (GHGs) by human activities, including carbon dioxide (CO_2), chlorofluorocarbons (CFCs), methane (CH_4), and nitrous oxide (N_2O) [1,2]. Among all the GHGs, CO_2 contributes dominantly to global warming [3]. Since the industrial revolution, the atmospheric CO_2 concentration has risen dramatically from approximately 280 ppm to over 415 ppm, largely due to fossil fuel combustion and industrial processes [4]. Projections indicate it may reach about 450 ppm by 2035, with energy-related emissions rising to 43.2 billion metric tons, potentially leading to a 2 °C increase in global mean temperature [5]. This trajectory risks severe environmental and economic consequences, including disruptions to ocean chemistry [6]. Therefore, global efforts to mitigate CO_2 emissions are critical, with targets aiming for significant reductions after 2030 and net-zero emissions between 2050 and 2060 [7].

More than 80% of the existing CO_2 in the atmosphere results from power plants, industrial facilities and transportation [8]. Thus, capturing CO_2 before its release into the atmosphere represents a crucial strategy for achieving decarbonization goals. To this end, various methods have been developed to capture CO_2, which can be classified into three categories, including pre-combustion, post-combustion and oxy-fuel combustion [9,10]. Among these, post-combustion capture—which separates CO_2 from flue gases after fuel combustion—is particularly amenable to integration with existing infrastructure, making it a widely adopted near-term solution [11–13].

To date, many technologies have been developed for CO_2 capture and sequestration, including absorption, adsorption, membrane separation, micro-algal bio-fixation, and cryogenic fractionation [14,15]. As summarized in Table 1, each method presents distinct trade-offs in cost, selectivity, maturity, and environmental impact. Chemical absorption, for instance, is a mature technology but suffers from high energy penalties for solvent regeneration, equipment corrosion, and environmental concerns [16–19]. Membrane and cryogenic processes often face challenges related to cost, energy intensity, or effectiveness at low CO_2 concentrations [20,21]. In this context, adsorption has gained considerable attention as a promising solid-phase capture technology. It operates based on the adhesion of CO_2 molecules onto a solid adsorbent surface via physical or chemical interactions, offering advantages such as lower energy consumption, reduced corrosiveness, and easier regeneration [22–24].

Table 1. A comparison of post-combustion CO_2 capture methods based on some key indexes.

Key Indexes	Capital/Operational Cost	Selectivity	Recovery	Reliability	Maturity	Environ. Friendliness
Absorption	High/high	Low-moderate	High (>90%)	Low (corrosion, solvent losses)	High	No (absorbent emission)
Adsorption	Moderate/moderate	High (specified adsorbent)	High (>90%)	High	Moderate	Very environmental-friendly

Membrane	High/moderate	High	Low-high (depending on the used membrane)	Moderate	Low	Relying on the type of membranes
Cryogenic	High/high	Low	Low	High	Low	Moderate
Bio-fixation	Low/high	High	Low	Low	Low	Environmental-friendly

The performance of adsorbents is largely governed by their textural properties (e.g., surface area, pore volume, pore size) and surface chemistry [25]. Consequently, porous materials with high surface areas and tunable pore structures are intensively investigated. Various adsorbents, including metal-organic frameworks (MOFs) [26], zeolites [27], oxide-based adsorbents [20], porous organic polymers (POPs) [28], porous polymer foams [29], and porous carbons derived from various precursors [8,16,30,31]. Numerous studies have been conducted primarily on the development of highly efficient adsorbents in terms of the adsorption capacity, energy efficiency/consumption, CO_2 recovery, operating conditions and costs.

Among these solid adsorbents, porous carbons attracted the most attention as the adsorbents for CO_2 capture [29], because they possess tunable pore structure and adjustable surface chemistry features that are suitable for CO_2 adsorption at both low and high pressures [32]. Usually, the adsorption of CO_2 by porous materials is mainly determined by the inherent properties of adsorbents, including the specific surface area (SSA), pore volume and size, and surface functional groups. Among these factors, the pore size is the key factor. It is recognized that porous materials rich in micropores or micro-mesopores are suitable for capturing CO_2 at either low- or high-pressures [33,34], respectively. Of course, the adsorption performance will be affected by the operating conditions. Compared with other adsorbents, porous carbons (mainly embodied as activated carbons) possess almost all the desired characteristics of an ideal CO_2 adsorbent, as illustrated in Figure 1. Furthermore, porous carbons have excellent water resistance, ensuring them a stable CO_2 adsorption performance under high humidity flue gas conditions, so that they can meet the requirements of practical applications. Accordingly, porous carbons become the most popular and effective CO_2 adsorbent [35].

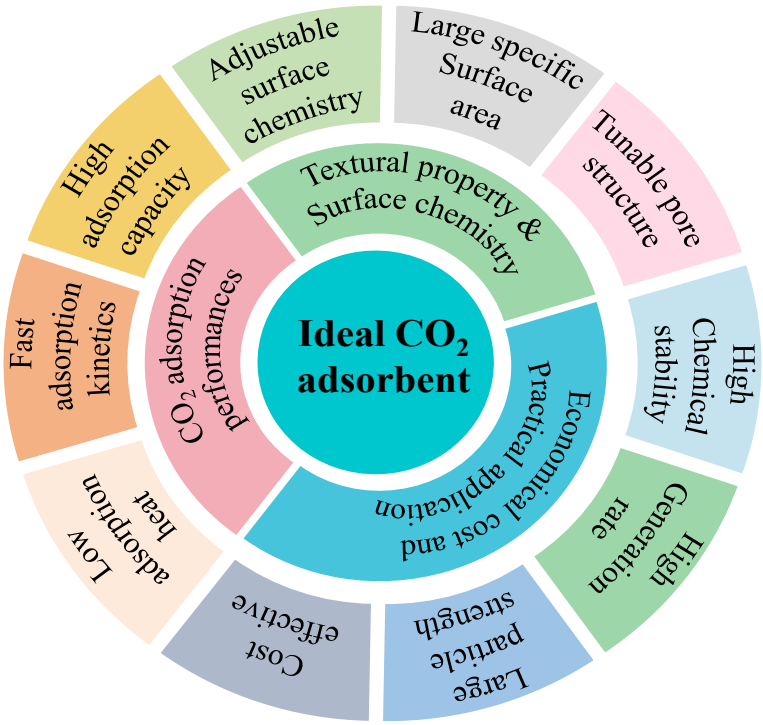

Figure 1. Desired characteristics of an ideal CO_2 adsorbent.

A few reviews have been published focusing on the utilization of porous carbons for CO_2 removal. These reviews provide a comprehensive overview of the existing porous carbons employed in CO_2 capture, including the preparation of porous carbon materials, the summaries of adsorption performance and the effects of operating condition factors [10,28,29]. These reviews are mostly biased towards the narrative and conclusive; none of them focus on the strategies for enhancing the adsorption capability of CO_2 capture in detail. For the researchers, understanding and mastering the strategies of how the modified porous carbons can enhance the CO_2 adsorption performance will be beneficial to the development of effective porous carbons for CO_2 capture. It is believed that a comprehensive and up-to-date review summarizing the recent strategies for enhancing the CO_2 adsorption performance of porous carbons is necessary, which can not only serve as a useful starting point for getting into one of the most important fields, but also facilitate the intensive research on the rational and efficient design and development of more effective porous carbons for CO_2 adsorption. Therefore, the present review aims to provide an overview of efforts to develop effective porous carbons for CO_2 adsorption via various strategies. While significant progress has been made in enhancing the gravimetric adsorption capacity of powdered carbons under ideal conditions, their transition to industrial-scale post-combustion capture requires addressing broader challenges, including the evaluation under real flue gas environments, the formation of robust pellets, and the integration with scalable adsorption processes like fixed-bed or circulating fluidized-bed systems [36]. This review starts with a brief introduction to CO_2 capture by adsorption. The second and third parts summarize the adsorption mechanism of CO_2 combined with the impacts of operation conditions on the CO_2 adsorption performance onto porous carbons. In the third section, the strategies to modify porous carbons for enhancing the CO_2 adsorption performance were thoroughly reviewed. The limitations, challenges and future prospects in the applications of porous carbons for CO_2 adsorption are addressed in the final section.

2. Mechanism of CO_2 Adsorption by Porous Carbons

The exceptional CO_2 adsorption performance of porous carbon materials (especially activated carbon) fundamentally stems from their unique disordered nanostructure. CO_2, possessing a strong quadrupole moment but no dipole moment, interacts with the carbon surface through polar bonds at both ends of its linear structure [29]. As a classic representative of non-graphitized (or "hard") carbon materials, activated carbon maintains a highly cross-linked microporous framework structure even under extreme temperatures (>2000 °C), thereby resisting graphitization. Modern structural studies utilizing advanced techniques, such as aberration-corrected transmission electron microscopy, reveal that this stability and its derived pore architecture originate from defect-rich sp^2 carbon networks. Contemporary models propose that its structure is not merely a simple stacking of minuscule graphene monolayers, but also incorporates non-hexagonal carbon rings (such as pentagons and heptagons) embedded within the matrix. These topological defects introduce persistent curvature, forming a complex three-dimensional network composed of ultramicropores (often slit-like) and defect sites [37]. It is precisely this intricate nanostructure—characterized by high specific surface area, tunable pore geometry, and chemically active defect sites—that underpins the physical and chemical adsorption mechanisms of CO_2 on porous carbon materials. The specific mechanisms have been thoroughly elucidated in relevant studies.

2.1. Physical Adsorption

The adsorption mechanism of CO_2 onto pristine porous carbon is illustrated in Figure 2. CO_2 capture by porous carbon is primarily controlled by physical adsorption or physisorption. In the mechanism of physical adsorption, the CO_2 molecules being adsorbed onto the surface of carbon sorbent mainly depends on the van der Waal's attraction between the CO_2 molecule and adsorbent surface, pole-ion and pole-pole interactions between the quadruple of CO_2 and the ionic, and the polar sites of the solid adsorbent surface

[33], which is verified from the reversible nature of the adsorption process. This adsorption process has a low heat ranging from −25 to −40 kJ/mole on carbon, which is comparable to the sublimation heat [34]. Even though the physisorption of the CO_2 molecule on the carbon surface could be temperature-dependent as it approaches equilibrium, namely, lower temperature is beneficial to more CO_2 being adsorbed, no activation energy is required for the occurrence of adsorption [38]. This is because of the linear shape and polar bonds on either end of CO_2, which can readily interact with the active sites on the carbon surface. In addition, both dispersion and induction contribute to the attraction of CO_2 to the carbon surface, correlating with the surface property [39]. Physisorption is recognized as an exothermic reaction with low enthalpy, owing to the weak Van der Waals attraction forces, and it is strongly dependent on the textural properties of the carbon material, such as specific surface area and micropore volume [40], while it is linked with adsorption energy. Beyond the classical Van der Waals forces, the intrinsic molecular properties of CO_2 play a pivotal role in physisorption within carbon frameworks. CO_2 possesses a significant quadrupole moment, which induces strong electrostatic interactions with the local electric fields generated by surface functional groups or structural defects. In ultramicropores (<0.8 nm), the overlapping potential walls from opposing pore surfaces significantly amplify these quadrupole-field interactions. This explains the enhanced CO_2 uptake at low partial pressures, as the energetic affinity of the pore system is dictated not only by pore volume but also by the electrostatic environment of the carbon matrix.

The adsorption performance of physisorption predominantly depends on the textural properties of carbon, facilitated by the intermolecular forces between activated carbon and CO_2. Porous carbon with a well-developed pore structure is crucial for CO_2 adsorption, and the primary texture parameters include specific surface area, pore volume, pore size, and its distribution, which determine the adsorption capacity of CO_2. Recent studies further emphasize the importance of hierarchical porous architectures derived from biomass waste for high-performance CO_2 capture [41]. Dai et al. [42] prepared rice husk derived porous carbon using KOH activation, having a specific surface area of 1496 m^2/g, total pore and micropore volume of 0.786 cm^3/g and 0.447 cm^3/g. This porous carbon exhibited CO_2 adsorption capacity of 5.83 mmol/g at 273 K and 1 bar and good CO_2/N_2 selectivity of 9.5. Deng et al. [43] fabricated bamboo derived porous carbon by KOH corrosion activation, which was rich in a lot of ordered micropores. The study disclosed that a perfect linear relationship existed between the pore size and CO_2 adsorption capacity, and the narrow micropores with a diameter of 0.55 nm were identified as the primary pores for CO_2 adsorption, exhibiting an adsorption capacity of 7.0 mmol/g. Silvestre-Albero et al. [44] investigated CO_2 adsorption onto carbon molecular sieves, and confirmed that CO_2 adsorption is not only related to the specific surface area, but is also strongly correlated with the micropore volume. Particularly, the developed, uniform and narrow micropores are the key to CO_2 adsorption. The significance of micropores of carbon materials in CO_2 adsorption was also validated by other studies [45–48].

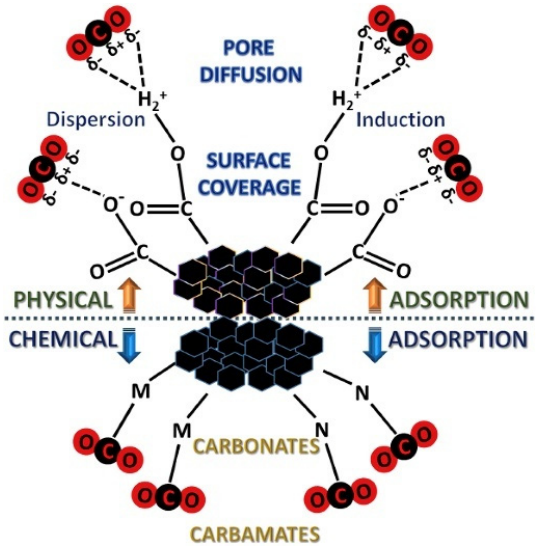

Figure 2. The adsorption mechanism of CO_2 on pristine porous carbon as an adsorbent. [Reproduced with permission from ref. [49], Copyright 2019, Elsevier].

Besides the textural properties, the chemical nature of carbon materials also plays a key role in CO_2 adsorption. The chemical nature can be defined by the heteroatoms present in their matrix, such as nitrogen, hydrogen, oxygen, phosphorus, and sulfur. These heteroatoms can originate either from the inherent compositions of the carbon precursor or the activation process introduced by the activating agent [50]. Specifically, the adsorption capacity and selectivity towards CO_2 depend on the surface functional groups formed by these heteroatoms and the delocalized electrons of the carbon structure. Detailed experimental and DFT studies have shown that the CO_2 adsorption capacity of N-doped carbons is governed by a threshold effect: at high nitrogen content, pyridinic-N (N-6) enhances localized polarity, whereas at low doping levels, pyrrolic-N (N-5) improves adsorption through conjugation effects [51]. Furthermore, studies combining experimental data with DFT calculations have recently unveiled the critical role of specific topological defects; for example, pentagonal topological defects were shown to work synergistically with N/O co-doping to enhance CO_2 adsorption by regulating the electronic distribution and promoting electron transfer on the biochar surface [52]. Among these heteroatoms, nitrogen (N) is the most popular heteroatom that is incorporated into the carbon matrix to improve the adsorption capacity and selectivity of CO_2 adsorption [29,53]. Recent DFT studies on Fe-N co-doped biochar have further demonstrated that the synergy between Fe and N generates Fe-N active sites, which enhance surface alkalinity and significantly boost CO_2 capture [54]. The introduction of nitrogenous groups like amide, nitrile, amines and others can increase the physisorption of CO_2 on carbon surface [29,48], due to the strong interaction between the acidic CO_2 and basic nitrogenous surface functional groups. The basic character of carbon is closely related to the resonation of π electrons present in carbon aromatic rings, which attract protons and nitrogen-containing groups. On the contrary, the acidic character of carbon is tightly linked with the presence of oxygen-containing groups, and the acidity will be greater when the oxygen concentration on the carbon surface increases.

2.2. Chemical Adsorption

In chemical adsorption of chemisorption, an acidic CO_2 molecule is attached to the active site on the carbon surface via covalent bonding. The chemisorption of CO_2 onto adsorbents can be evaluated by characterizing the used carbon after adsorption and by identifying the heat of adsorption. During the adsorption process, the CO_2 gas undergoes a covalent chemical reaction to connect with the specific active sites on carbon, with a substantially high adsorption heat that is almost equal to the heat of reaction [34]. Compared with physisorption, chemisorption has a much higher heat of adsorption, ranging from 40–400

kJ/mol [55], owing to its strong chemical bond. Moreover, CO_2 is adsorbed on the carbon surface and chemically bonded to form carbonates. Generally, CO_2 chemisorption is irreversible. The formed carbonates usually include bicarbonate, bidentate carbonate, and monodentate carbonate, which correspond to weak, medium, and strong adsorption basic sites [47].

Chemical adsorption of CO_2 by porous carbon is generally accomplished through doping various heteroatoms onto porous carbons. The most frequently adopted methods include doping nitrogen, comprising urea, melamine, p-Phenylenediamine, polyethyleneimine, polyaniline, *etc*. Nitrogen-containing functional groups can lead to chemisorption via the formation of a zwitterion or a carbamate, and the hydration of CO_2 to form bicarbonate [38]. Tan et al. [39] investigated the adsorption of CO_2 on nitrogen-doped porous carbon prepared from licorice residue and urea, revealing a synergistic effect between the nitrogen content and the activated carbon's structure on CO_2 adsorption performance. They found that nitrogen content contributed remarkably to CO_2 adsorption, attributed to the acid-base reaction between CO_2 and doped nitrogen atoms. CO_2 is recognized as a weak Lewis acidic gas that can react with doped nitrogen-containing groups that act as Lewis bases due to their negatively charged and electron-donating behavior [42]. The chemical interaction between N-containing functional groups and CO_2 involves more than simple acid-base neutralization. For amine-functionalized or N-doped carbons, the reaction typically follows a zwitterion mechanism. In the absence of moisture, a CO_2 molecule undergoes nucleophilic attack by the lone pair of electrons on the nitrogen atom to form a zwitterion intermediate, which subsequently undergoes proton transfer to form a stable carbamate: $2RNH_2 + CO_2 \leftrightarrow RNHCOO^- + RNH_3^+$. Under humid conditions, the mechanism shifts towards a bicarbonate pathway, where water acts as a proton mediator, theoretically doubling the stoichiometric capture capacity per nitrogen site: $RNH_2 + CO_2 + H_2O \leftrightarrow RNH_3^+ + HCO_3^-$. In addition, Wang et al. [44] examined the adsorption performance of CO_2 on a series of nitrogen-doped porous carbon, and an enhanced CO_2 adsorption capacity was observed. The nitrogen species, such as pyridine-N, pyrrole-/pyridine-N, graphitic-N, pyridine-N-oxide and primary/secondary amines, can react with CO_2, forming graphitic-N, carboxyl groups and heterocyclic structures (pyrrolic-N), thus facilitating the CO_2 adsorption. This is corroborated by a recent study on N, S co-doped porous carbon derived from coconut shell, where the presence of pyridinic-N and pyrrolic-N significantly contributed to a high CO_2 uptake of 4.38 mmol/g at 25 °C, demonstrating the critical role of these N-functionalities in enhancing surface basicity and Lewis acid-base interactions with CO_2 [56]. In addition to nitrogen, other atoms, for example, oxygen, sulfur, boron, phosphorus, *etc*., can be doped and facilitate the chemical adsorption of CO_2 on heteroatom-doped porous carbon materials.

Apart from heteroatom doping, metal impregnation on carbon has been demonstrated to have excellent stability and prominent adsorption enhancement, especially via chemisorption. Numerous studies have clearly proved that the impregnation of metal ion into biomass derived porous carbon can integrate their multiple advantages effectively, leading to a much-enhanced CO_2 adsorption performance [45–47]. The presence of metal ions will result in the formation of bidentate and monodentate carbonates owing to the bonding between CO_2 and metal ions (Mg^{2+}) and/or O^{2-} [48]. In addition, the strength of basic sites of carbons is proportional to the amount of coordinated electronegative metal ions, which can be boosted by employing metal-impregnated carbon with a high specific surface area, providing more space for O^{2-} sites [50]. More importantly, the impregnation of metal ions can greatly improve the adsorption capacity of CO_2 under humidity. Generally speaking, the presence of H_2O will significantly inhibit the adsorption of CO_2 onto carbon [57]. While for metal-impregnated carbons, for example, MgO-based and $Mg(OH)_2$-based carbons are capable of generating $MgCO_3$ in the presence of H_2O [58], thereby improving the CO_2 adsorption capacity. The water vapor will serve as a channel for enhanced chemisorption interactions between MgO and CO_2, producing CO_3^{2-} and H^+ ions when water surrounds MgO. Besides magnesium ions, other metal ions can be impregnated into carbon to enhance the chemisorption of CO_2 onto carbon, which will be discussed in detail later.

The adsorption mechanism of CO_2 onto carbon materials can be summarized in Figure 3, involving both the physical adsorption promoted by the porous structures and chemisorption induced by doping heteroatoms or impregnating metal ions. Carbon materials will continue to undergo extensive investigation in CO_2 adsorption; some challenges, including low adsorption efficiency, high operation expenses and weak moisture/impurities tolerance, should be addressed. Hence, elucidating the adsorption mechanism is very crucial to the theoretical exploration and industrial applicability of carbon materials for CO_2 capture.

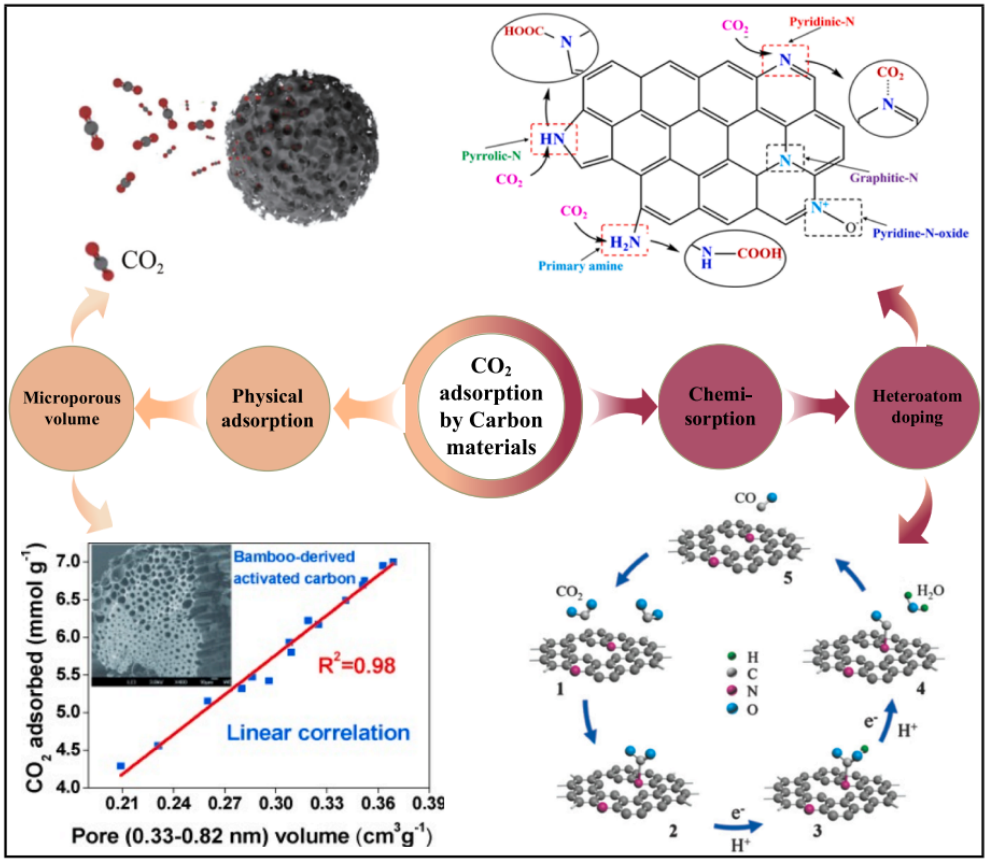

Figure 3. The adsorption mechanism of CO_2 onto porous carbon materials by physical and chemical adsorption with various kinds of interactions [Reproduced with permission from ref. [31], Copyright 2024, Elsevier].

3. Impacts of Operation Conditions on CO_2 Adsorption

The CO_2 capture in actual applications is carried out in various kinds of complicated conditions, and the operating parameters will inevitably influence both the capacity/extent and rate of CO_2 adsorption. The typical operating parameters include temperature, partial pressure of CO_2, water vapor, and impure gases (NO_x, SO_x, H_2S, *etc.*). It is necessary to review and clarify the impacts of CO_2 adsorption on porous carbons, for developing appropriate adsorbents that can effectively work under these conditions and still have high adsorption capacity.

3.1. Adsorption Temperature

The adsorption temperature exercises an important influence over the adsorption performance from both physical and chemical adsorption [59,60]. The variation of temperature itself possesses a propensity for either negative and positive (sometimes conflicting) effects on individual aspects of CO_2 adsorption. On one hand, adsorption is exothermic, so it is predicted that the CO_2 adsorption capability increases as the adsorption temperature decreases [61]. On the other hand, CO_2 molecules have high kinetic energy at high temperatures, so they can move faster, resulting in less adsorption time on the adsorbent surface, which

leads to reduced adsorption capacity. Although the increased energy enables a greater diffusion rate of gaseous molecules, the possibility of CO_2 being adsorbed or retained on the carbon surface by fixed energy adsorption sites is decreased. As shown in Figure 4a, the CO_2 adsorption capability of sugarcane bagasse derived carbon decreased linearly (R^2 = 0.93) with the increase of temperature, which confirms a strong negative correlation between CO_2 adsorption capacity and adsorption temperature.

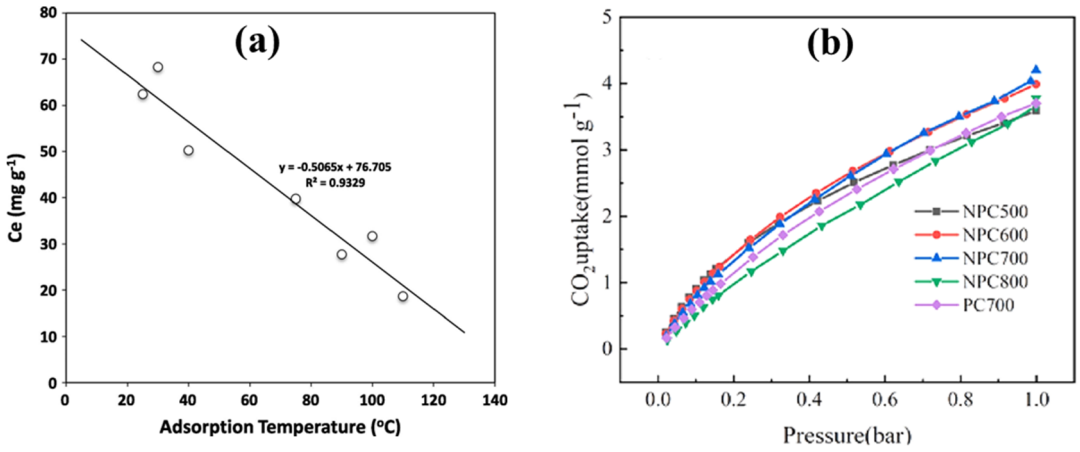

Figure 4. (**a**) Effect of temperature on CO_2 adsorption of sugarcane bagasse derived carbon [29], (**b**) CO_2 adsorption isotherms of nitrogen-doped porous carbons (NPCs) and porous carbons (PC) at 25 °C in the pressure range of 0–1 bar [62].

3.2. Adsorption Pressure

There is a considerable demand for more studies on the adsorption capacities of carbon materials at higher pressures. Numerous researches have proved that the operating pressure plays a significant effect, and CO_2 adsorption capacity increases with the elevation of CO_2 pressure [63–65]. As shown in Figure 4b, the porous carbon and nitrogen-doped porous carbon all exhibited enhanced CO_2 adsorption capacity with the elevation of pressure ranging from 0 to 1.0 bar, and the maximal CO_2 adsorption capacities of 3.59–4.20 mmol/g were obtained at 25 °C and 1.0 bar [62]. When a gas molecule is adsorbed onto a solid surface, the global volume of the adsorbent will decrease. According to Le Chatelier's principle, the equilibrium state will shift toward a new state when a stress (for example, a change in pressure) is applied on a system, and the new state will counteract the applied stress. To counter the increase in pressure, the number of gas molecules in the system tends to be reduced, thereby the adsorption capacity of CO_2 on the adsorbent will increase [66,67].

Furthermore, the investigation on the adsorption capacity at varied pressures can gain insights into the role of each materials property of porous carbons on CO_2 capture capacity. The previous studies demonstrated that CO_2 capture capacity at low pressure of 0.1–0.2 bar was more correlated with the practical post-combustion application [47,55], which was consistent with the partial pressure of CO_2 in flue gas. In fact, the CO_2 capacity on porous carbon is determined synergistically by the adsorbent properties (such as textural properties and chemical compositions) and the operating conditions, while their impacts are not independent. To determine the underlying dependent relationships between CO_2 adsorption capacity and adsorbent properties and operating conditions, machine learning (ML) methods were recently adopted, which can identify complex nonlinear relationships among multiple influencing factors and interdependent variables. Shang et al. [59] developed robust ML models to predict the CO_2 adsorption capacity of porous carbon based on the adsorbent properties and adsorption conditions. They found that pressure played a dominant role in determining CO_2 adsorption capacity at low pressure (0–0.2 bar), while the relative contribution of pressure declined with increasing pressure. In addition, the textural properties are more vital to CO_2 adsorption than chemical composition across different pressure and temperature ranges; the relative importance of ultra-micropores increased with increasing pressure.

3.3. Water Vapor

In actual CO_2 capture, water is one of the most frequent impurities in the gas stream, especially, water vapor is ubiquitous in the flue gas and in lots of other CO_2-rich industrial gases. H_2O is usually the third most abundant component in flue gases after N_2 and CO_2, followed by O_2. The water content in flue gases is 6–18% depending on the origin [60], while it is typically 6–7% in biogas [61]. H_2O can be strongly adsorbed by many inorganic adsorbents, for it is a polar molecule, so the presence of H_2O in the mixture can cause some problems for adsorbents. For example, competitive adsorption will occur between CO_2 and H_2O, and the adsorption capacity for CO_2 will be weakened for the adsorbents that have a higher affinity toward water molecules than CO_2 molecules [68,69]. For this reason, a dehumidifying unit was proposed for H_2O removal from the feed gas prior to entering the capture unit, such as inserting a layer of a moisture adsorbent material (e.g., alumina, alumina-zeolite) [70,71]. Nevertheless, the dehumidification units will increase the overall capital and operating costs [72,73]. Although carbon adsorbents are hydrophobic, showing fewer issues with water vapor, it is still required to study the humidity effect on carbon adsorbents for CO_2 adsorption, given the ubiquitous nature of water in gas streams.

Porous carbons generally exhibit type-I adsorption isotherm for CO_2, indicative of their high affinity toward CO_2 at low partial pressures [74]. Moreover, they often show low affinity toward water vapor at low relative humidity (RH) with low adsorption capacity, while the water uptake increases dramatically at higher RH levels, which is reflected as the "S"-shape adsorptions corresponding to type-V isotherm [75,76]. It is recognized that water adsorbs first over surface functional groups due to its strong affinity for water, then on top of the chemisorbed water molecules via hydrogen bonding, based on the model proposed by Do and Do [77]. Eventually, water clusters will form on the surface of porous carbons and move into their micropores, as established earlier based on experimental and theoretical results [78–80]. Subsequently, the generated water clusters contributed to micropore filling within the adsorbent, potentially occupying the micropores completely, leading to competitive adsorption between the water and the target gas (CO_2).

Most investigations on carbon-based adsorbents carried out under subatmospheric pressures reported negative impacts of humidity on CO_2 uptake, as a result of the competitive adsorption with water. Duran et al. employed one commercial carbon (Norit R) and two biomass-derived porous carbons for CO_2 adsorption from a flue gas stream, and single-component adsorption isotherms of N_2, CO_2 and H_2O were measured to evaluate the selectivity of CO_2 to water and nitrogen at 30–70 °C [81]. They found that water was adsorbed preferentially on all the carbon samples compared with CO_2, especially at the lowest temperature. When 2 vol% H_2O/N_2 and 2 vol% H_2O/8 vol% CO_2/N_2 gas mixtures corresponding to 48 and 16% RH at 30 and 50 °C was used, water uptake was hardly affected by CO_2. On the contrary, the presence of water reduced CO_2 uptake remarkably at the highest RH, and the prehydration of the adsorbents at 30 °C reduced CO_2 uptake by as much as 46%. For the biomass-derived porous carbons, their surface functionality is a determining factor for water adsorption in terms of hydrophobicity and hydrophilicity. How the surface hydrophobicity of biochar varies with the feedstock and preparing conditions is controversial based on the reported studies. Some proposed that the hydrophobicity changed with the activation method [82] and the increase of production temperature [83–85]. The details are discussed as follows.

Younas et al. [82] investigated the influence of activation method on the competitive adsorption of water vapor and CO_2 onto a palm shell derived porous carbon, and both physical activation and chemical activation using 20–50 wt% NaOH solutions were used to prepare porous carbons. They found that the presence of water vapor (20% RH) can reduce CO_2 uptake, and the negative effect of humidity was more severe for physically than chemically activated porous carbons, with 45% and 13% declines, respectively. Gray et al. [83] inspected the influences of porosity and hydrophobicity of biochar on water uptake. The biochar was produced from two feedstocks (hazelnut shells and Douglas fir chips) at three production temperatures (370, 500 and 620 °C). The production temperature changed the surface hydrophobicity, and

the hydrophobicity decreased with an increase in the production temperature, which can be ascribed to the volatilization and loss of the aliphatic functionality at higher production temperatures. Contrary to the studies by Gray et al., some other works reported opposite results, where the hydrophobicity increased with increasing production temperature. These studies assessed hydrophobicity by measuring atomic ratios such as O/C, H/C and (O+N)/C [86,87] raising the pyrolysis temperature would result in the reduction of both ratios [88], leading to a subsequent increase in hydrophobicity due to the loss of the polar functional groups.

At high pressure, there is an extensive consensus regarding the beneficial effect of water on CO_2 adsorption onto carbon adsorbent. Zhou et al. [89] measured CO_2 adsorption isotherms of coconut shell derived microporous carbon at 275 K up to 40 bar over prehydrated adsorbents. The moisture content R_w, was defined as the ratio of adsorbed water to carbon. Figure 5a revealed that the moisturized samples had lower CO_2 uptake than the dry carbon at low pressure, and their CO_2 uptake increased significantly at 15 (20 bar), while the CO_2 uptake on dry carbon was almost stable over 15 bar. This was ascribed to the enhanced solubility of CO_2 in water at high pressure, resulting in the formation of CO_2 hydrate. Figure 5b demonstrates that the inflection point occurs at higher pressure as temperature increases, and the point values are comparable to the pressure required for the formation of CO_2 hydrate in pure water. Unlike that on the exclusively microporous carbons, the CO_2 adsorption isotherms over micro-/mesoporous carbons showed similar transitions in the presence of water, but no plateau was observed with the formation of CO_2 hydrate [29].

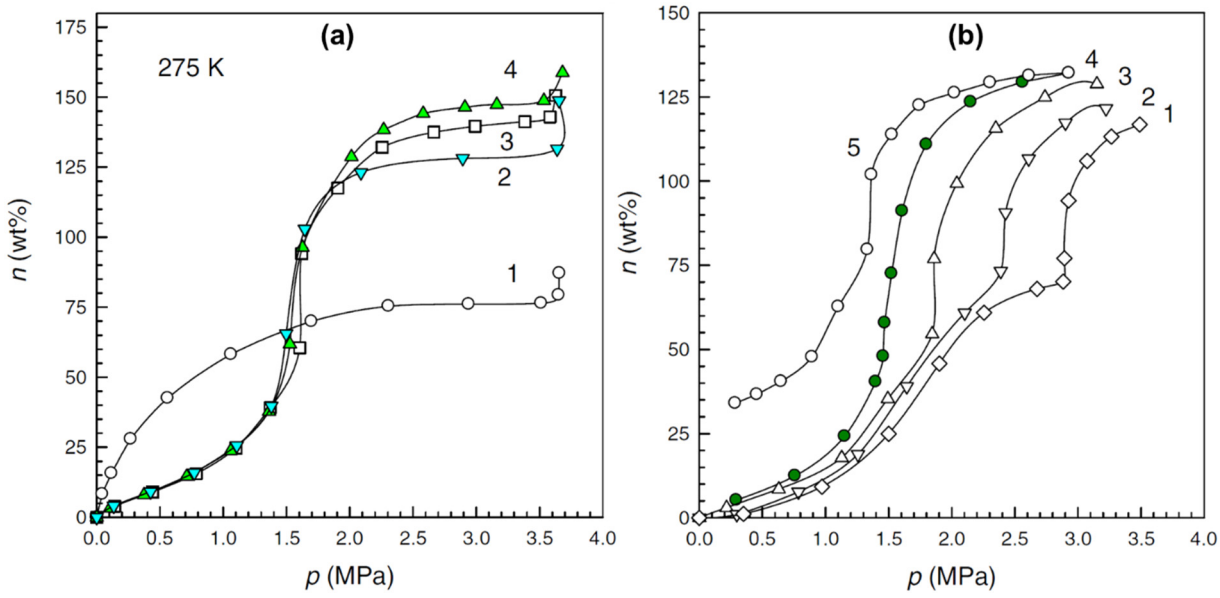

Figure 5. CO_2 adsorption isotherms on a microporous carbon (**a**) with different moisture contents at 275 K. 1: R_w = 0, 2: R_w = 1.74, 3: R_w = 1.32 and 4: R_w = 1.65; (**b**) different temperatures under R_w = 1.31. 1: 281 K; 2: 279 K; 3: 277 K; 4: 275 K (adsorption); 5: 275 K (desorption). [Reproduced with permission from ref. [89]. Copyright 2007 Elsevier].

3.4. NO_x, SO_x, H_2S, CH_4

Numerous studies available have focused on the adsorption of pure CO_2 on carbon adsorbents [90–92], while CO_2 is hardly produced as a pure component. In addition to the mentioned water vapor, there are other gas impurities, including NO_x, SO_x, H_2S and CH_4, which also can influence the adsorption efficiency of CO_2 onto carbon adsorbents [93]. Usually, NO_x and SO_x in the gas stream will react with or be adsorbed on the adsorption sites, forming complexes with adsorbed compounds, leading to a decrease in the number of sites available for the adsorption of the CO_2 molecule. Accordingly, clarifying the impacts of these impurities on CO_2 adsorption is essential to determine the feasibility of an effective adsorbent [94].

NO_x is a byproduct produced during fuel combustion, which can be adsorbed by porous carbons via primarily chemical process, depending on the presence of oxygen in the flue gas instead of the structural properties of the adsorbents. Zhang et al. [95] investigated the NO adsorption onto different porous carbons with various pore structures and surface functional groups. They found that virtually no NO can be removed in the absence of oxygen, while a large amount of NO was removed rapidly through adsorption and oxidation facilitated by porous carbons that acted as both adsorbent and catalyst. The NO_x removal can be enhanced on the metal-loaded and heteroatom- doped porous carbons. Chen et al. [96] studied NO adsorption on ordered mesoporous carbon (OMC) and cerium loaded OMC, finding that oxygen played the key role in NO adsorption, and physical adsorption was the main mechanism of NO removal without oxygen. Additionally, the OMC displayed twice the NO adsorption capacity as the disordered porous carbon, and the introduction of cerium into the OMC enhanced the NO adsorption.

The adsorption of SO_x on carbon materials is principally dependent on physical adsorption facilitated by the porous structure and chemical adsorption by surface alkaline functional groups on carbon. Sun et al. [97] inspected the adsorption of SO_2 on activated carbon and carbon nanotube, finding that SO_2 was mainly adsorbed in the micropores, since the micropores contained strong potential energy fields enabling SO_2 to be easily adsorbed onto carbon. A wide pore size distribution is not beneficial to the generation of adsorption potential energy fields, the SO_2 adsorption will be reduced. Sethupathi et al. [98] examined the adsorption performances of CO_2, H_2S and CH_4 by four different biomass derived porous carbons produced from perilla leaf, soybean stover, Korean oak and Japanese oak, and the adsorption tests were conducted in a continuous fixed bed. The porous carbons exhibited negligible adsorption of CH_4 even without any of the other gases, which was attributed to the large pore size (>1 nm) allowing CH_4 molecules to slip. All the carbons exhibited good adsorption performance for pure CO_2 and H_2S, while the adsorption capacities toward CO_2 decreased by 90–95% when the gas mixture was employed. This was because of the competitive adsorption between CO_2 and H_2S, where H_2S was preferred to be adsorbed. It can be concluded that the acidic gases such as H_2S can inhibit CO_2 adsorption on carbon surface.

Great progress has been achieved in dealing separately with the three common acidic gases found in flue gas, namely CO_2, SO_2 and NO_x, while there is less research on simultaneously removing these three acidic gases through adsorption. On the other hand, it is crucial to understand the mutual influence among the three gases in the adsorption process to improve the adsorption capacity, especially for capturing CO_2 in the presence of other acidic gases. Zhou et al. [63] investigated the co-adsorption behaviors of CO_2, SO_2 and NO that exist in flue gas onto porous carbon by experimental measurement and theoretical model fitting. They found that the Freundlich model was more accurate than the Langmuir model in predicting the adsorption amount, the adsorption affinity of porous carbons towards the three gases followed the order: $SO_2 > CO_2 > NO$, and the sequence of required work was as follows: $CO_2 > NO > SO_2$. These findings provide some theoretical foundation for removing CO_2 by adsorption onto carbon adsorbent in the presence of other acidic gases.

Yi et al. [64,65] examined the simultaneous adsorption of CO_2, SO_2 and NO on metal-loaded porous carbons. It was found that the Cu-loaded carbon showed better adsorption performance than those porous carbons loaded with other metals such as Ca, Mg and Zn, and the adsorption capacities were 0.367, 0.357 and 0.090 mmol/g for CO_2, SO_2 and NO, respectively. Furthermore, they found that high temperature impacted negatively the adsorption of these gases and low temperature favored their adsorption on porous carbon. The adsorption capacity of SO_2 and NO can be improved in the presence of oxygen, and the oxidation of them into SO_3 and NO_2 would be promoted by oxygen. Moderate amounts of water vapor can enhance the adsorption capacity of SO_2, while reducing the adsorption of CO_2 and NO owing to their low solubility in water. Finally, the adsorption mechanisms of CO_2, SO_2 and NO are illustrated in Figure 6. The acidic gases, including CO_2, SO_2 and NO, can be adsorbed simultaneously over carbon materials. However, the main adsorption mechanism toward them varied to some extent. Among them, CO_2 is primarily

adsorbed by physical adsorption, while SO_2 and NO are adsorbed mainly by chemical adsorption. Up to now, limited research has been conducted on the simultaneous adsorption of them. Therefore, overcoming the mutual influence of these gases during the adsorption process remains both necessary and challenging. Initial insights into such complex interactions come from studies on binary gas mixtures relevant to flue gas compositions. For instance, research on the co-adsorption of CO_2 and acetone (a model VOC) on N-doped biochar revealed an initial competitive adsorption followed by a synergistic phase where acetone enhanced CO_2 uptake, likely through dissolution and capillary condensation effects, while CO_2 itself inhibited acetone adsorption [99]. It is expected to achieve satisfactory removal results by selecting suitable loading and doping functional groups on carbon materials.

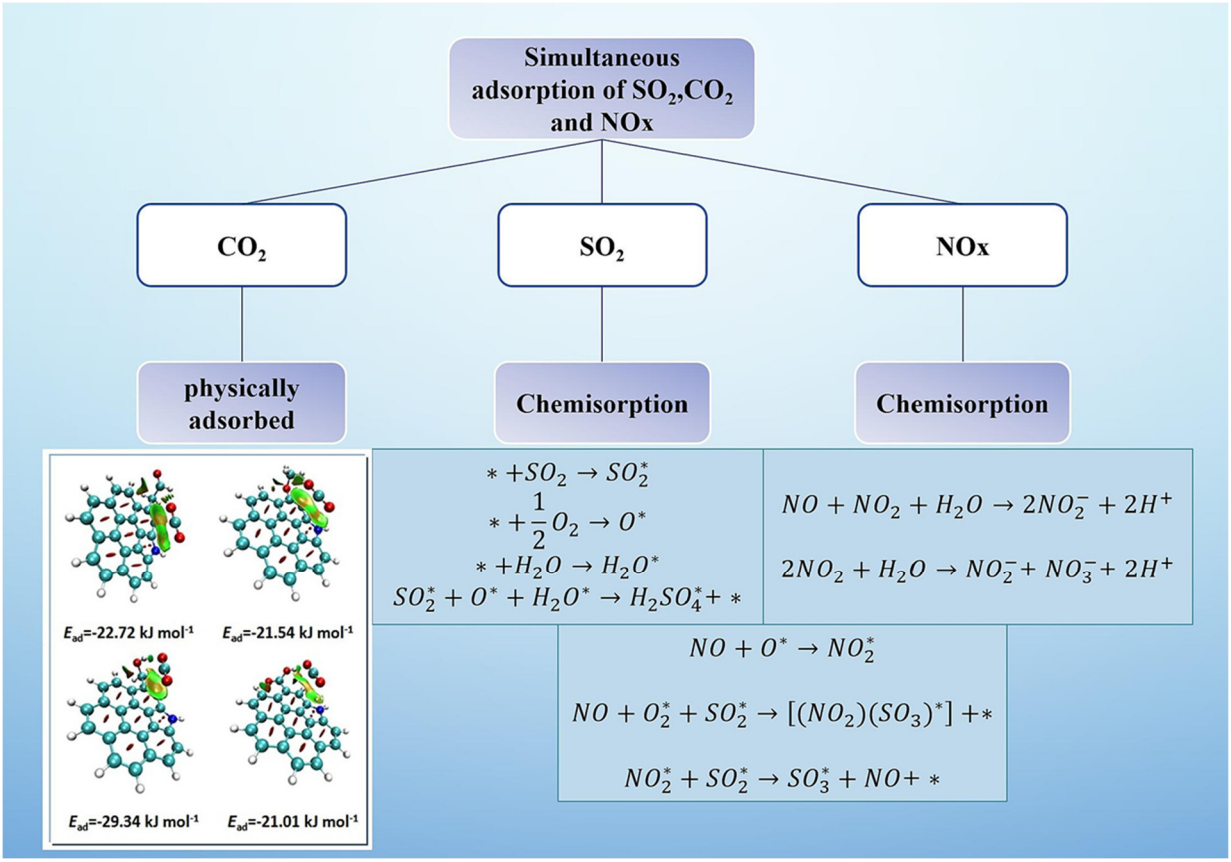

Figure 6. Mechanism of simultaneous adsorption of CO_2, SO_2 and NO_x by carbon adsorbents. [Reproduced with permission from ref. [100,101]. Copyright 2019 ACS publications, 2014 Springer]. The "*" symbol denotes an adsorption site.

4. Strategies for Enhancing CO_2 Adsorption on Porous Carbons

4.1. Tuning Porosity

The textural properties of porous carbon adsorbents are the dominant factors that determine their adsorption performance towards CO_2 capture. The pores in porous carbons can be classified into micropore (pore size/width (d) < 2 nm), macropore (d > 50 nm) and mesopore (2 nm < d < 50 nm), relying on the size of the pore. It is generally recognized that the adsorption of small molecules like CO_2 is principally dependent on the micropore filling mechanism, and the CO_2 adsorption capability of porous carbon is mainly correlated with the narrow microporous structure [102,103]. Previous studies have verified that micropores with a size less than 1 nm, especially ultra-micropores (d < 0.8 nm), are much more beneficial to CO_2 uptake at ambient pressure [104,105], and they can improve the selectivity of CO_2 to N_2 [106]. As an ideal adsorbent, additional properties besides the adsorption capacity, *i.e.*, good regeneration ability, rapid adsorption kinetics, stability, *etc*., are key to the adsorbents in practical applications [107,108].

Although the mesopore and macropore in porous carbons contribute a little to the adsorption capacity of CO_2, they supply channels for rapid diffusion of CO_2 and are beneficial to the desorption; then the porous carbon materials in the absence of mesopores usually have poor regeneration ability [109]. In this regard, continuous efforts have been devoted to tuning the pore structure of carbon adsorbents with appropriate hierarchical pore size and pore size distribution for improving their CO_2 adsorption performance.

How to fabricate porous carbon with a suitable pore structure has been the focus of research in the CO_2 adsorption by porous adsorbents. The fabrication of porous carbon generally requires two steps: carbonization, in which the raw materials are graphitized and activation for tuning the porosity. The overall number of pores, the shape and size of pores, as well as the pore size distribution, determine the adsorption capacity, as well as the adsorption rate. The carbon materials by merely carbonizing the raw materials usually have little pores, which are averse to CO_2 adsorption. Some carbonized products have higher porosity, but their pore size distributions are not ideal, in which the pore diameter/width is bigger than the pore size required for CO_2 separation with poor selectivity, on account of the heterogeneous composition and structure of the carbon-containing raw materials. To render the as-fabricated porous carbons show better adsorption performance for CO_2, it is vital to further tune the pore structure after carbonization by various activation methods. Activation control is commonly used to tune the pore size of porous carbon, which can make the pore structure much more developed by opening or expanding the pores.

Chemical activation by using KOH, K_2CO_3, $ZnCl_2$, *etc*., as activating agents is one of the most effective pore creation and regulation methods. Beyond traditional chemical activators, innovative media such as molten salts have been employed to achieve uniform and deep micropore development. For instance, a one-step molten salt thermal treatment using a NaOH-Na_2CO_3 system was shown to effectively integrate carbonization and activation, producing N/O co-doped biochar with a high specific surface area (up to 3312.89 $m^2 \cdot g^{-1}$) and a well-developed microporous network, leading to a CO_2 uptake of 6.02 $mmol \cdot g^{-1}$ at 273 K and 1 bar [110]. Deng et al. [111] fabricated porous carbons derived from peanut shells and sunflower seed shells using KOH as an activating agent, and the optimal porous carbons were achieved at a low KOH/C ratio of about 1.0. The porous carbons derived from the two precursors exhibited CO_2 uptake of 1.54 and 1.46 mmol/g at 298 K and 0.15 bar. Though the peanut shell derived porous carbon had much lower surface area and micropore volume than the sunflower seed shell derived porous carbon, it showed higher CO_2 uptake owing to its higher volume of micropores in the range of 0.33–0.44 nm. Moreover, the volume of micropores with a width of 0.33–0.44 nm had a linear relationship with the CO_2 uptake, demonstrating that these micropores were responsible for CO_2 adsorption. Many more studies reported that porous carbons with a pore size of 0.7–0.9 nm possess the maximal CO_2 adsorption capacity rather than the larger pores ($d > 1$ nm) [43,112–114]. Recently, Liu et al. [115] further identified that the advantageous ultramicropores (0.6–0.8 nm) in N-doped biochar played a decisive role in CO_2 uptake. The pore size in carbon can be roughly controlled by adjusting the carbonization temperature and activation process, while the design and synthesis of efficient porous carbon with a suitable micropore size requires more sophisticated means, which include choosing a proper precursor, performing an appropriate pre-treatment method and activation process.

Tang et al. [116] prepared porous carbon by selecting date sheets as carbon sources, combined with controllable carbonization and subsequent KOH activation. Figure 7a shows the synthesis procedure. The date sheets have the natural internal open pores consisting of thin laminates, which can be tailored towards promoting the activation step. The fresh date was first pre-treated with washing, impurity removing and cutting into small sheets, and the reprocessed date sheets were freeze-dried overnight for 48 h and designated as FDDS (freeze-dried date sheets). The FDDS were carbonized at 500 and 800 °C obtaining CDS-500/800, and the CDS were activated by pyrolysis of the mixture of CDS/KOH with a certain ratio to achieve ACDS. Figure 7b,c display the N_2 isotherms and corresponding PSD plots. These isotherms and PSDs demonstrated that the pore structure varied significantly with the mass ratio of KOH to CDS. All the

samples have type-I isotherms with a high N_2 uptake at a low relative pressure ($P/P_0 < 0.1$) and a wide adsorption knee and plateau, indicative of the microporous structure. As the KOH/CDS increased from 2 to 6, the adsorption knee became wider, suggesting the production of more mesopores. This study disclosed that the temperature had less impact on the pore structure, as the temperature increased from 500 to 800 °C, the N_2 isotherms, PSDs and the textural parameters did not change much, maybe due to the carbon source and freeze-dried pre-treatment. Figure 7d exhibits the CO_2 adsorption isotherms over all the date derived carbon samples. It can be observed that the CO_2 adsorption capacities of all activated samples are obviously higher than those of the mere carbonized samples without activation. The ACDS-500-2 has a CO_2 adsorption capacity of 5.98 mmol/g, which is close to ACDS-800-2 and ACDS-800-4 with values of 6.0 and 6.4 mmol/g at 0 °C. Figure 7e shows the typical adsorption isotherms toward CO_2 and N_2 at 25 °C on ACDS-800-4, demonstrating the good selectivity (41.53) of ACDS-800-4. The relationship between the pore size and CO_2 uptake in Figure 7f revealed that a good linear relationship existed as the pore size was in the range of 0.7–0.9 nm, and the pores with a size of 0.5–0.7 nm play a major role in CO_2 adsorption. The adsorption of CO_2 has the optimized energy [117], when the pore size is two or three times of a CO_2 molecule (ca. 0.33 nm).

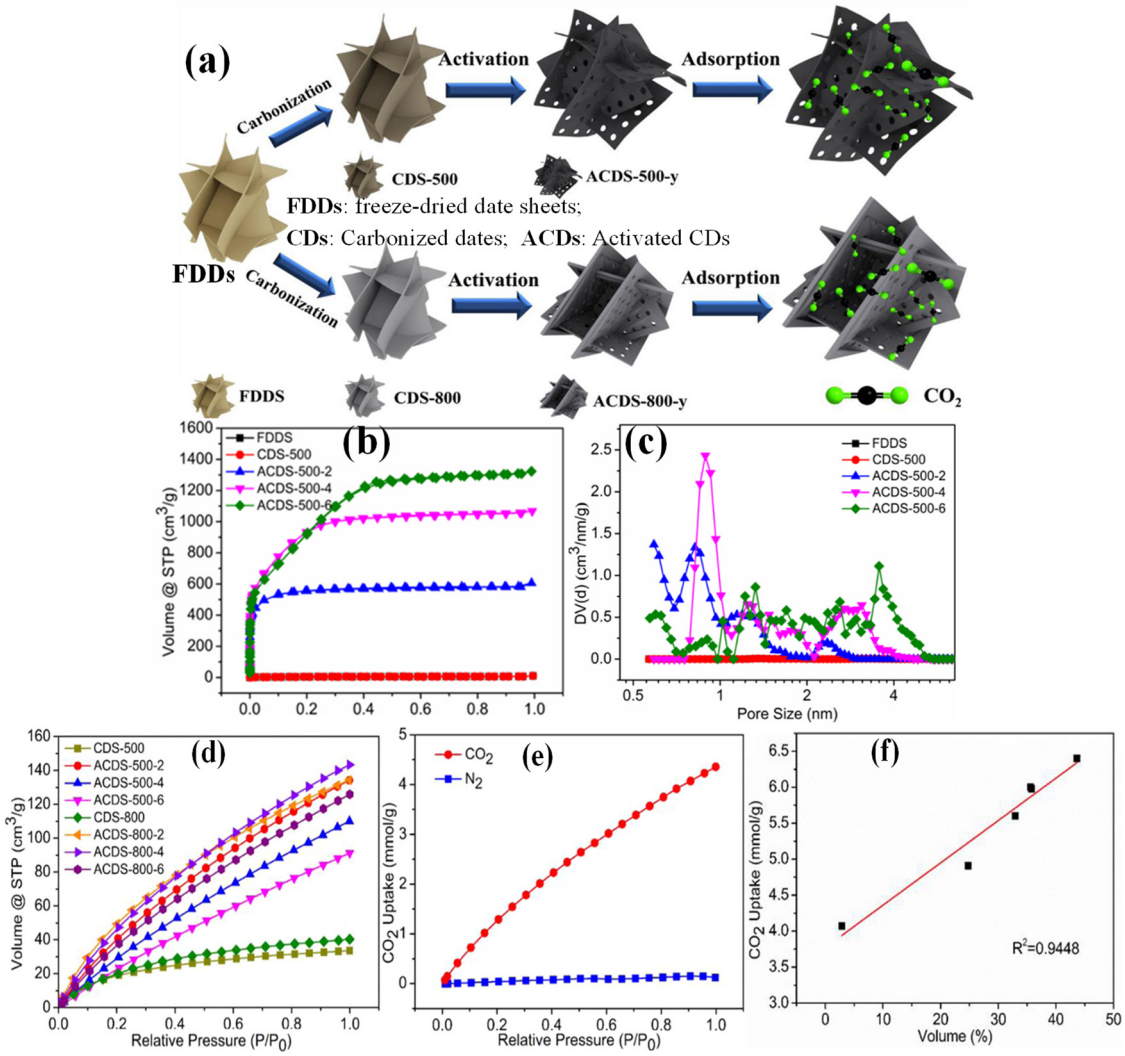

Figure 7. (**a**) Illustration of the syntheses of CDS-x, ACDS-500-y and ACDS-800-y from FDDS; (**b**) N_2 adsorption/desorption isotherms and (**c**) pore size distributions (PSDs) plots of FDDS, CDS-500; (**d**) CO_2 adsorption isotherms of all samples at 0 °C and 1 bar, (**e**) CO_2 and N_2 adsorption isotherms at 25 °C and (**f**) Correlations between the amount CO_2 uptake and proportion of cumulative pore volume of pores with pore size of 0.7–0.9 nm of ACDS-800-4. [Reproduced with permission from ref. [116]. Copyright 2019, Elsevier].

Up to now, most studies focused on enhancing the CO_2 gravimetric adsorption performance onto porous carbons with low packing density, which can cause the insufficient utilization of pores rich in porous carbons. On the other hand, CO_2 adsorption capability per volume of porous carbons can provide a relatively realistic indication of their performance, compared with the gravimetric performance. Additionally, the volumetric CO_2 adsorption capability of porous carbon is an essential indicator for assessing the efficiency and scale of adsorption systems [118–120], whereas it is often overlooked in the field of CO_2 capture by adsorption [102,121]. For the sake of obtaining porous carbons with high volumetric CO_2 adsorption capacity, porosity regulation of carbon is a prerequisite because the pore configuration and size can influence remarkably the packing density of porous carbons [122]. In order to develop desirable porous carbon with high volumetric CO_2 adsorption capacity, Qie et al. [123] employed a simple chemical activation using K_2CO_3 as the activating agent to prepare coal-derived porous carbons. Figure 8a displays the fabrication process of coal-derived porous carbons and the formation mechanism. By simply varying the pyrolysis temperature from 600 to 900 °C, the porosity in the coal-derived carbons can be controlled. As illustrated, the ultra-micropores obtained at 600–700 °C in the resulting porous carbons gradually grew into micropores and meso-micropores at 800 and 900 °C, respectively. Figure 8b,c shows the N_2 adsorption-desorption isotherms and the correlation between the CO_2 uptake and the PSDs. The obtained ACs were used as a CO_2 adsorbent, revealing the importance of ultramicropores for CO_2 uptake. The ultra-microporous carbon (AC-600) with a high packing density exhibited the highest volumetric capacity of 1.8 mmmol/cm^3 at 0 °C. Their experimental results and molecular dynamic simulation disclosed that CO_2 adsorption capacities increased linearly with the micropore volume, whereas the volumetric capacities were directly proportional to the ultra-micropore volume.

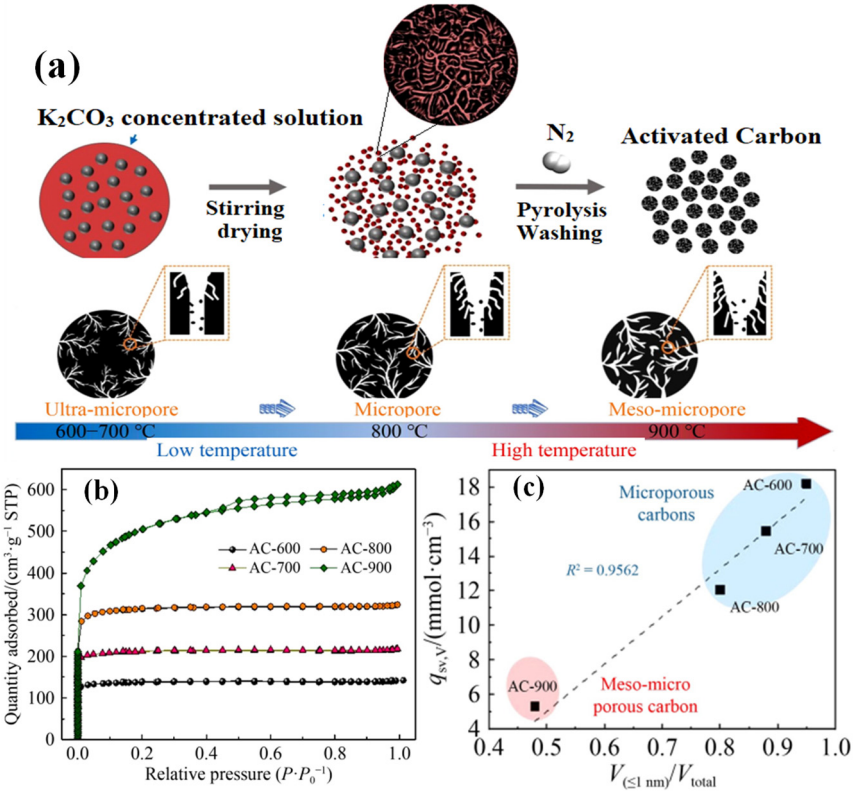

Figure 8. (**a**) Schematic illustration of the fabrication of coal based activated carbon (AC) by K_2CO_3 activation and the corresponding pore formation mechanism in the ACs; (**b**) N_2 adsorption/desorption isotherms of the ACs prepared at different activation temperatures; (**c**) Correlations between the amount CO_2 uptake per volume and $V_{(d \leq 1\ nm)}/V_{total}$) of the ACs at 0 °C. [Reproduced with permission from ref. [123], Copyright 2022, Springer].

Chemical activation has advantages in preparing porous carbons, for example, the obtained porous carbons usually have a high specific surface area and abundant micropores, and the operating temperature is low (<900 °C) [124]. On the other hand, it has obvious shortcomings, which are the use of strong alkali or acid in the activation process, which will cause low carbon yield, corrosion to the instruments and environmental pollution. Apart from chemical activation, physical activation is often used to tune porosity in carbon materials. Physical activation has been well commercialized for the production of coal or biomass derived porous carbon. Specifically, in the physical activation process, oxidizing gases (*i.e.*, H_2O, CO_2, O_2, *etc*.) are often used as the activation agents to generate pores, in which small volatile molecules first release from the carbon matrix forming the initial pores at low-/medium temperature, then the gas activation agents gradually etch the carbon framework from the surface to inside to create desirable porosity. This process usually involves the reactions: $C + H_2O \rightarrow H_2 + CO$ (−131 kJ) or $C + CO_2 \rightarrow 2CO$ (−170.5 kJ) at varied temperatures (ca. 700–1000 °C) [124,125]. Relatively, physical activation is environmentally friendly, while it wastes a lot of carbon. The main strategy of regulating the pore structure of carbon by physical activation is to adjust the reaction atmosphere [126], for example, choosing a proper activating agent and temperature, due to the diversity in molecular size, diffusivity and reactivity of the activation agents. Recently, microwave pyrolysis has been shown to be an efficient alternative for fabricating porous carbons with uniform pore structures and high specific surface areas, owing to its inward-to-outward heating mode, which reduces pore blockage and promotes pore development [127]. However, the porous carbons obtained by physical activation generally have low specific surface area (less than 1000 m^2/g) and low pore volume (<0.5 cm^3/g), because of the low reactivity between gaseous activation agents and carbon framework, so the adsorption performances are usually unsatisfactory.

In view of the weaknesses of a sole physical or chemical activation method, it is necessary to develop low-cost, facile and effective strategies for tuning porosity in carbon. Catalytic activation is a promising method, referring to the addition of metal compounds to a carbon source to increase the surface-active points. To tune the porosity of coal-derived carbons and reduce the dosage of activation agents, Sun et al. [128] proposed a green and efficient strategy for preparing porous carbons, namely, a trace K_2CO_3 induced catalytic CO_2 activation system. In their strategy, a small amount of K_2CO_3 was added (less than 2% weight ratio of coal), which can prominently reduce the reaction barrier between the CO_2 molecule and the coal framework, facilitating the pore formation of the coal-derived porous carbons. The resulting coal-based porous carbon using trace K_2CO_3 has short range ordered microcrystalline structure and developed pore structure with a high specific surface area of 1773 m^2/g and pore volume of 1.11 cm^3/g, even superior to the porous carbon using a large dosage of K_2CO_3 (K_2CO_3/C=3), and was three times more than those samples from solely CO_2 activation. They found that the potassium-base component (mainly C–O–K structure) embedded in the coal matrix can act as a catalyst for intense erosion reaction between coal and CO_2 molecule, which was generated during a CO_2 atmosphere at high temperature and can enhance the pore formation in the resulting porous carbons. When used as a CO_2 adsorbent, the trace-K_2CO_3 catalyzed porous carbon exhibited high CO_2 adsorption capacity with value (4.36 mmol/g at 0 °C) and good adsorption-regeneration cycling stability.

4.2. Surface Modification

In addition to textural properties, the surface chemical structure of porous carbon has been verified to affect CO_2 adsorption capability significantly [126,129–132]. The chemical property depends on the type and number of surface functional groups, which affect the interaction between CO_2 and the porous carbon. As discussed above, the adsorption capacity toward CO_2 will decrease with increasing temperature, but can be enhanced prominently by chemical modification. For example, when basic groups are introduced into the surface of porous carbon, the modified porous carbon will show stronger interaction with CO_2 than the pure porous carbon, due to the introduced basic sites having intermediate affinity to CO_2. Of course, the

affinity is inadequate to induce chemical adsorption for CO_2 [133]. The enhancement of the interaction between the adsorbent and CO_2 molecules can be realized by various kinds of surface modification techniques. The modification techniques for porous carbon include physical, chemical or microbiological methods, which are very important because they can change the physical structural properties or surface chemical functional groups [134], so as to enhance the CO_2-adsorbent interaction. The direction of these modifications is pore functionalization by introducing polar groups, for instance, nitro, hydroxy, amine, sulphonate, imine, *etc*. [129]. These surface functional groups (SFGs) can be introduced either prior to adsorbent synthesis by judicious selection of modification of the precursors, where CO_2-philicmoieties will form during the synthesis procedure, or alternatively via post-synthesis modification when functional groups are introduced and attached to the surface of carbon.

Heteroatomic doping is a frequently used strategy to modify the surface chemical properties of pristine carbons. For most pristine porous carbons, their CO_2 adsorption capacities are less than 3 mmol/g at atmospheric pressure [113], which is attributed to the limited active sites mainly derived from defects on the surface of adsorbents. Heteroatom doping usually involves the introduction of nonmetal element into the carbon matrix, and it is one of the most efficient ways to generate defects, in that the doped heteroatoms have similar atomic radius, orbit, electronegativity and charge density with carbon atoms that can change the electron and surface charges of the final materials [132–134]. Various kinds of heteroatoms have been successfully doped into porous carbons, for example, N, B, O, S, P, *etc*., obtaining higher CO_2 adsorption capacity and selectivity compared with the unmodified counterpart [135]. The enhancement is primarily attributed to increased electrostatic interactions with acid-type gases, such as CO_2.

As an adjacent element to carbon, nitrogen bears several similar chemical properties and atomic size with carbon [136], and can generate relatively stable chemical bonds with carbon [137]. Due to such similarities, introducing nitrogen will theoretically the electron density of the carbon framework or increase the basicity, which will in turn anchor the electron deficient carbon of CO_2 to the carbon pore surface via Lewis acid-base (N atom) interactions [138]. Therefore, nitrogen is the most investigated heteroatom doped in carbon materials [139], since nitrogen atoms can easily enter the carbon skeleton without causing a serious lattice mismatch. Nitrogen-doped carbons generally refer to the modified carbon matrix where few carbon atoms are replaced by nitrogen atoms, being enriched with diverse types of nitrogen bearing functionalities on their surface. The possible nitrogen species and nitrogen functionalities formed on carbon surface are illustrated in Figure 9. The typical nitrogen species on carbon surface include pyridinic, pyridonic, pyrrolic, graphitic or quaternary nitrogen, combined with amine, nitro, nitroso and amide type. The amine functionalities consist of all the primary, secondary and tertiary amine. Apart from quaternary nitrogen, the other types of N-functionalities formed at the edge site of the graphitic plane, creating more defects than the undoped carbon.

Generally speaking, doping nitrogen via post-synthesis (activation) method will decrease the specific surface area and pore volume, for the introduced N in the carbon skeleton can lead to blocking of the earlier developed pore structure, which is disadvantageous to the CO_2 adsorption capacity. However, the introduction of N can result in a considerable decrease in the amount of surface acidic groups and an increase of surface basic groups due to the generated nitrogen functionalities. Specifically, nitrogen functionalities on the carbon surface provide a lone pair of electrons, so they can act as the attractive sites for the electron-deficient carbon atom of the CO_2 molecule owing to the high electron-withdrawing properties of oxygen atoms [136]. Moreover, the basicity of nitrogen-doped carbon can strengthen the dipole-dipole interactions and hydrogen- bonding to the surface, leading to an increase in the selectivity over non-polar gases such as N_2 and CH_4 [137,138]. On the other hand, the polar nitrogen functional groups will improve the hydrophilicity of carbon, and the H_2O molecules are usually trapped inside the narrow micropore of carbon on account of the enhancement in hydrogen bonding with H_2O [131,139,140]. Thus, the nitrogen-doped porous carbons may be better suited to the adsorption removal of CO_2 in the dry flue gas.

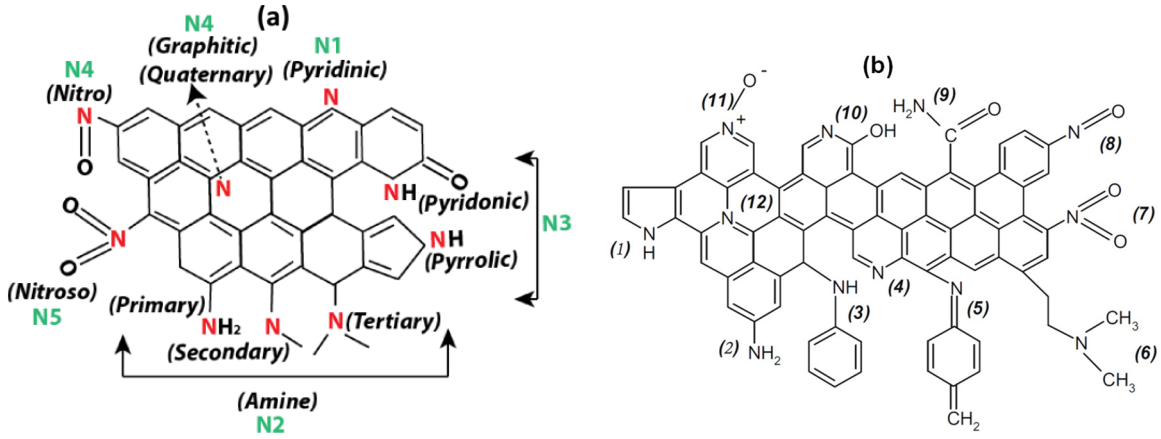

Figure 9. (**a**) Nitrogen species on doped carbon surface via NH_3 activation (Reproduced from Ref. [131], with permission from Elsevier), (**b**) Various types of nitrogen functional groups on coal-derived nitrogen-doped carbon: (1) pyrrole, (2) primary amine, (3) secondary amine, (4) pyridine, (5) imine, (6) tertiary amine, (7) nitro, (8) nitroso, (9)amide, (10) pyridone, (11) pyridine-N-oxide, (12) quaternary nitrogen (Reproduced from Ref. [140], with permission from Elsevier).

Nazir et al. [141] fabricated N-doped porous carbons utilizing polyacrylonitrile (PAN) as carbon source and $NaNH_2$ as both porogen and nitrogen supply during carbonization. The resulting optimized "PN-3" sample had satisfactory textural features with SSA of 2490 m^2/g and pore volume of 2.06 cm^3/g, together with nitrogen content of 6.4 at.%. The experimentally measured CO_2 uptake for all the N-doped porous carbons ranged from 5.17 to 7.15 mmol/g at 273 K/1 bar, from 4.13 to 5.59 mmol/g at 283 K/1 bar. It also exhibited an excellent CO_2/N_2 selectivity (~102) based on the ideal adsorbed solution theory at 273 K, surpassing the performance of most undoped porous carbons. Additionally, the CO_2 adsorption process was driven by physisorption, indicated by the relatively low isosteric adsorption heat of 39.10 kJ/mol and low activation energy of 5.05 kJ/mol. Wang et al. [142] synthesized nitrogen-doped porous carbons through carbonization of ZIF-8 and ZIF-61 assisted by KCl and NaCl, showing a highly microporous structure and high nitrogen content. Their results demonstrated that the cumulative pore volume in the pore size of 5–7 Å, pyrrolic-N content and COOH content played favorable influence on CO_2 adsorption capacity. The evaluation by a multiple linear regression equation confirmed that the optimum pore structures ($V_{5–7Å}$ > 0.10 cm^3/g) and pyrrolic-N were the dominant contributors to CO_2 adsorption capacity. The highest CO_2 adsorption capacity of 4.61 mmol/g at 298 K and 6.70 mmol/g at 273 K can be acquired with a high CO_2/N_2 selectivity of 39.5 under typical flue gas and cycling stability.

Besides PAN and ZIF, other precursors have been utilized to prepare nitrogen-doped carbon via *in-situ* method. Liu et al. [143] transformed oxytetracycline fermentation residue into an *in-situ* N-doped nanoporous carbon by low-temperature pyrolysis coupled with pyrolytic activation. They found that the mild activation conditions (600 °C, KOH/carbon = 2) resulting in micropore-rich porous carbon with high *in-situ* nitrogen content, and the doped nitrogen in the carbon skeleton with high oxygen enhanced electrostatic interactions facilitating the CO_2 adsorption. The maximal adsorption capacity arrived at 4.38 and 6.40 mmol/g at 298 and 273 K and 1 bar, with high CO_2/N_2 selectivity (32/1) and favorable Q_{st} (33 kJ/mol) as well as excellent reusability (decreased by 4% after 5 cycles). Wu et al. [144] produced nitrogen-doped porous carbons from bamboo shoot shells using urea as a nitrogen source, activated by potassium carbonate. Their results revealed that the as-produced N-doped porous carbon exhibited a fibrous structure and distinct worm-like microporous structure, and the largest specific surface area was 1985 m^2/g with a nitrogen content of 1.98 at.%. The optimized sample demonstrated outstanding capacity of CO_2 adsorption with values of 7.52 and 3.60 mmol/g at 273 and 298 K under 1 bar, and it also exhibited excellent cyclic stability and CO_2/N_2 selectivity. The thermodynamic calculations verified that the CO_2 adsorption process

on nitrogen-doped biochar was spontaneous and exothermic, indicative of its physical adsorption. Furthermore, Zhang et al. [145] utilized fir sawdust as a precursor, employing urea and thiourea as nitrogen and sulfur sources with a secondary activation strategy to yield micropore-rich carbon. The resulting material showed high selective CO_2 capture with an uptake of 3.96 mmol/g at 298 K and 1 bar and a CO_2/N_2 selectivity of 47.

Like nitrogen, boron is an adjacent element to carbon with similar chemical properties and atomic size to carbon [141], so the spatial structure of B-doped carbon materials will not change significantly [142], while there are more active sites on the B-doped carbon surface with enhanced adsorption performance due to the uneven electron distribution on their surface [143]. By contrast, boron loses electrons while nitrogen gains electrons to form relatively stable chemical bonds with carbon (BC_3), suggesting that the carbon atoms adjacent to boron show different electronegativity from those adjacent to nitrogen [146]. Li et al. [147] investigated the influence of boron-doped porous carbon on the CO_2 adsorption performance. Their results demonstrated that the B atom played a beneficial role in the CO_2 adsorption process, and the B-doped carbon with a B/C ratio of 0.05 exhibited the highest CO_2 adsorption performance with 2.16 mmol/g at 303 K and 1 bar. Through in-depth analysis, it is found that boron presents some contradictions in the adsorption performance of B-doped carbons. On one side, boron doping can create useful active sites and the boron-doped carbon has some Lewis basicity, which is advantageous to the interaction with CO_2 molecules having weak Lewis's acidity. On the other hand, the oxygen affinity of boron means the boron-doped structure is easily oxidized, and the Lewis alkalinity of the oxidized structure is weakened that impair the CO_2 adsorption performance. Thus, it requires further exploration of how to form stable boron-doped carbon for improving CO_2 adsorption performance of B-doped carbon.

Oxygen is often doped into the carbon skeleton to improve the CO_2 adsorption performance, because oxygen is the next most frequent element to carbon, and the oxygen-containing groups can contribute to determining the hydrophobicity/hydrophilicity and acidity/basicity of carbon adsorbents. Figure 10 shows the common oxygen-containing functional groups [146], which are traditionally divided into two categories according to their acidic or basic character. It is well-recognized that carboxyl groups, lactones, phenol and lactol groups account for the acidic character of carbon materials. While there are controversies on the basic groups, chromone, ketones and pyrones were proposed as the basic O-containing functionalities [147,148]. The pyrone-like groups at the edges of the carbon surface could be the most important basic functionalities. The pristine carbon is usually hydrophobic, so the degree of hydrophilicity is often decided by the amount of polar O-groups [130]. Unfortunately, the increase of hydrophilicity is not conducive to CO_2 adsorption, since it enhances the adsorption of moisture in the flue gas, leading to the reduction of active adsorption sites toward CO_2. Even so, the oxygen functionalities can improve the adsorption properties of carbon toward CO_2. For example, an increase of 26% in CO_2 uptake has been reported on the oxidized phenolic resin derived carbon compared with the unmodified carbon [149].

Generally, O-containing functionalities are produced from the oxidation of organic structures during various kinds of chemical/physical activation procedures [150]. Acidic groups are formed at relatively low temperatures under oxidization with HNO_3, H_2O_2, H_3PO_4 or H_2SO_4 [151]. More strong surface basicity could be introduced by NaOH activation than H_3PO_4 at the same temperature of 850 °C. The basic groups can be more effectively introduced by activation with H_3PO_4 in the presence of steam than in an inert (N_2) atmosphere [152], and extreme activation conditions were shown as detrimental to the formation of surface functional groups [153]. The surface O-containing groups of porous carbon have electron-rich properties, which can strengthen the interactions between the CO_2 molecule and carbon surface owing to the introduction of various polar groups [154]. Bai et al. [155] modified activated carbon fibers (ACFs) by liquid oxidation with hydrofluoric acid to introduce O-containing functional groups. The liquid-oxidized ACF had 112% higher CO_2 adsorption capacity than those observed onto the pristine ACFs. The enhancement was attributed to the synergistic effects of developed pores and the O-functionalities that

guide CO_2 into the micropores via the attractive forces exerted on the electrons in CO_2 molecules. Then they concluded that the introduction of carboxylic and hydroxyl surface groups was effective in improving CO_2 adsorption performance.

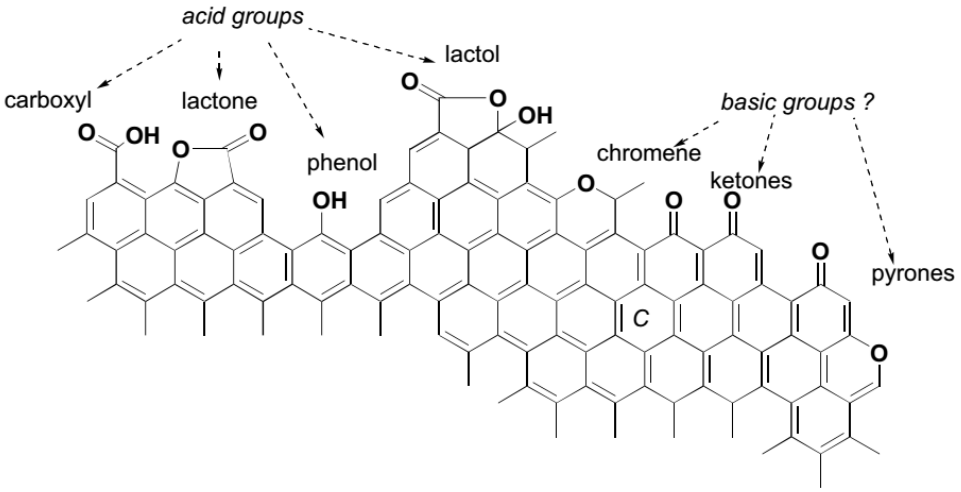

Figure 10. Possible basic and acidic oxygen functionalities on carbon surfaces. (Reproduced from Ref. [146], with permission from Elsevier).

As for the enhancement of CO_2 adsorption by oxygen-doped carbon, there are some different reports. Tiwari et al. [156] thought the high content of O-containing basic groups contributed to the highest CO_2 adsorption capacity of the epoxy resin-derived carbons. Babu et al. [157] found aht the CO_2 adsorption capacity increased with the oxygen concentration, and postulated that both –OH and –COOH groups facilitated the considerable improvements in CO_2 adsorption capacity at ambient pressure. As mentioned above, nitrogen-containing groups can present Lewis basic character of carbon materials. Beyond that, the oxygen-containing groups also have a similar function. O-groups like ethers, alcohols and carbonyls comprise electron-donating oxygen atoms, which participate in the electrostatic interactions with the CO_2 molecule [149,158], then improving the adsorption of polarizable species such as CO_2 by Lewis acid-base interactions [159]. Among the basic oxygen functionalities, pyrone is often investigated, and pyrone-like structures are the combinations of non-neighboring carbonyl and ether-O at the edges of a graphene layer [146]. The basicity of pyrone originated from the stabilization of its protonated form via electronic π-conjugation throughout sp^2 skeleton of the carbon basal plane [130,160]. –OH group is often reported as basic and affects the adsorption of CO_2 due to its high electron density [161,162]. The interactions between –OH groups and the CO_2 molecule mainly depended on the hydrogen-bonding and high electrostatic potential [163,164]. A linearity between CO_2 adsorption capacity and the content of oxygen groups was observed at 298 K below 0.5 bar, while it was not found when the adsorption pressure was increased from 0.5 to 1 bar.

Sulfur is also frequently doped in carbon materials to improve their application performances. Compared with N, O and B atoms, sulfur is much larger in size so that it can protrude out of the graphene plane, resulting in the increased graphite layer spacing, the distortion and deformation and a large amount of strains and defects within the carbon skeleton [130,165]. These defects and strains can alter the original charge distribution, inducing charge localization, so that more active sites will be produced in the S-doped carbons that are conducive to CO_2 adsorption [166]. Additionally, S-doping can increase the reactivity owing to the lone-pair electron donation of the sulfur atom [167]. Xia et al. [168] reported that the S-doped carbons exhibited higher CO_2 uptake capacity than the S-free carbon, which was ascribed to the strong pole-pole interactions between the large quadrupole moment of CO_2 molecules and polar S-groups associated with sites. Seem et al. [169] found a linear relationship between CO_2 adsorption capacity and

the quantity of oxidized-S in the S-doped porous carbons, and the S-doped microporous carbons were more effective than similarly prepared N-doped samples in CO_2 adsorption. Density Function Theory (DFT) calculations revealed that the interaction of CO_2 with sulfoxides and sulfones was stronger than those with N-moieties, according to the calculated binding energy.

Phosphorus is another heteroatom extensively doped in carbon materials. Phosphorus belongs to the nitrogen group and is also electronegative, having similar chemical property with nitrogen, doping phosphorus into carbon will alter the electron density of carbon structures, producing some active sites [170,171]. Different from nitrogen, phosphorus has a larger atomic size, thus the formation of the C–P bond will increase the spacing of the graphite layer, leading to further changes in density [172]. Up to now, there are few reports on phosphorus dope carbon materials applied in CO_2 adsorption, so the corresponding enhanced adsorption mechanism is rarely reported and not clear. Zhou et al. [171] investigated the CO_2 capture by several carbon phosphides with the assistance of an electric field, finding that the carbon phosphide acting as a CO_2 adsorbent had good CO_2 capture performance. However, a recent study on N and P co-doped porous biochar has successfully demonstrated enhanced CO_2 capture performance under conventional conditions and provided a detailed synergistic mechanism analysis focusing on the tuning of nitrogen species and active sites [173]. Accordingly, it is necessary to conduct further investigations to understand how the atomic charge of phosphorus and the spatial structure of phosphorus doped carbon affect the CO_2 adsorption.

4.3. Metal Impregnation

Another modification of porous carbon is metal modification, and numerous reports have clearly indicated that the impregnation of metal ions onto carbon can combine their respective multiple advantages, resulting in great-enhanced CO_2 adsorption performance [174–176]. In fact, metal oxides are often employed as adsorbents independently for CO_2 adsorption in industrial applications, due to their acid-base and redox properties. Unfortunately, there are some limitations for the usage of metal oxide alone in CO_2 adsorption, for example, low surface area and poor stability. Impregnating metal oxide can increase the oxygen groups on the surface of porous carbons, serving as a metal oxide anchoring site, which facilitates the CO_2 adsorption by tailoring the basic characteristics of porous carbons. Metal oxide impregnated porous carbon (MPC) has excellent mechanical features due to the size quantization effect, especially towards CO_2 [177], and a great number of active sites for CO_2 adsorption will be generated. Therefore, MPCs have been employed to improve CO_2 adsorption ability; various kinds of metals, including sodium (Na), Calcium (Ca), magnesium (Mg), nickel (Ni), *etc*. have been introduced into porous carbons for improving CO_2 adsorption capability of porous carbons [153,178].

MPC can effectively adsorb CO_2 via physical and chemical sorption over a wide temperature from 473 K to 673 K, and low energy is required for CO_2 regeneration [179]. Othman et al. [180] incorporated four different types of metal oxides into activated carbon nanofibers (ACNF), such as magnesium oxide (MgO), manganese dioxide (MnO_2), zinc oxide (ZnO) and calcium oxide (CaO) by electrospinning and pyrolysis process. They observed the ACNF with MgO incorporation exhibited the largest surface area of 413 m^2/g and the highest CO_2 adsorption of 60 cm^3/g at 298 K and 1 bar. Similarly, Lahijani et al. found that a Mg based MPC showed a higher CO_2 adsorption potential (82.0 mg/g) than raw activated carbon (72.6 mg/g) [153]. In addition, cyclic CO_2 capture experiments demonstrated that porous carbon containing basic metals had a higher capacity for CO_2 adsorption because it can react with acidic CO_2 molecules. MPC impregnated with Mg via $Mg(NO_3)_2$ salt yielded 3.1 mmol/g CO_2 adsorption, while MPC with Mg-sugarcane via $MgCl_2$ salt achieved CO_2 adsorption capacity of 227–235 mg/g [176]. The plain TiO_2 showed a comparably limited CO_2 adsorption capacity verified by the isothermal experiments [181], and the highest CO_2 adsorption capacity was only 3.1 mmol/g at 313 K, even up to 25 MPa. Likewise, Tungsten (VI) oxide (WO_3), as an earth-abundant metal, has a low CO_2 adsorption capacity of 0.3 mmol/g at 313 K that is lower than that of

TiO_2 [182]. Fortunately, impregnating TiO_2 or WO_3 into carbon can improve the CO_2 adsorption affinity, as the doping procedures and composites of metal oxide-carbon increase the Lewis basicity, allowing their better adsorption of Lewis acidic CO_2 [183]. Especially, the addition of an oxygen-rich surface functionality of porous carbon to the WO_3 lattice can improve the CO_2 adsorption, implying a better affinity toward CO_2.

Table 2 summarizes the porous carbons modification with impregnation of various kinds of metal oxides, for example, MgO, NiO, CuO, *etc*. All these results have indicated that the impregnation of metal oxide onto porous carbon surely enhanced the CO_2 adsorption capacity compared with the raw carbons. On the other hand, there are also some reports that the CO_2 adsorption capacity was reduced as metal oxides were impregnated into porous carbons.

Table 2. Summary of CO_2 adsorption performance of porous carbon impregnated with different metal oxides.

Adsorbent Materials		S_{BET} (m^2/g)	Adsorption Conditions		CO_2 Uptake (mmol/g)	Change of Perf. (%)	Refs.
Carbon Precursor	Metal Oxides		Temp. (K)	Pres. (bar)			
Coconut shell	MgO	976	298	1	2.63	50.3	[184]
Commercial Activated carbon	NiO	925	298	1	2.73	10.1	[185]
	MgO	820	298	1	2.68	8.1	
Activated carbon	CuO	1974	303	1	6.78	124.5	[186]
Mesoporous carbon	MgO	298	353	1	5.45	-	[187]
Charcoal	CaO	63.6	298	1	15.1	-	[188]
Carbon nanofiber	NiO	331	298	1	2.40	-	[189]
Hickory chips	FeOOH	-	298	1	3.64	much	[190]
Activated carbon	Cu/Zn	599	303	100 kPa	2.25	48.0	[191]
Walnut shell	MgO	292	298	1	1.86	12.9	[153]
Carbon nanofiber	MgO	413	298	1	1.38	-	[180]
Activated carbon	γ-Fe_2O_3	833	298	1	2.47	27.1	[192]
Activated carbon	CuO	1277	303	100 kPa	2.11	28.7	[193]

Li et al. [194] modified porous carbon by multiple metal oxides, such as CeO_2, CuO, NiO and Mn_3O_4 with varied weight loadings of 10–30%. They investigated them as adsorbents for CO_2 capture, observing that the overall CO_2 adsorption capacity decreased upon metal oxide modification. They attributed this to the reduction in the total surface area of the porous carbon/metal oxide composite. As a matter of fact, the surface area of metal oxide is far below that of porous carbons, so the total surface area of the composite will usually be decreased due to the covering of the surface by metal oxides, especially under an excess amount of metal oxides impregnated. Luckily, the CO_2 adsorption capacity of MPC at a relatively low-pressure range (below 0.4 bar) increased with high metal oxide loading (30%), particularly for NiO modified MPC, owing to the stronger interaction strength between CO_2 and metal oxides than with the carbon surface. In addition, the CO_2/N_2 selectivity values of MPC are generally higher than those of the pristine porous carbons, and the 30% NiO-modified MPC exhibited 72% increase in the selectivity, which is ascribed to an increased interaction between CO_2 and the introduced metal oxides supporting by the increased isosteric heats of CO_2 adsorption for MPC. The decrease in CO_2 adsorption capacity onto MPC was also observed on ACNF@metal oxide composites. Othman et al. [180] impregnated MgO, MnO_2, ZnO and CaO into ACNF via electrospinning method. They found that only MgO impregnated MPC showed slightly higher CO_2 adsorption capacity than that of pristine ACNF, due to the decrease of S_{micro} percentages in these MPCs.

As a composite, the adsorption performance of MPC is inevitably determined by the dosage of metal impregnated on the MPC, especially for the ratio and type of metal precursor, as well as the amount of MPC in the CO_2 adsorption process. Generally, metal impregnation modifies the surface chemistry of parent carbons, and the active adsorption sites will increase when metal is incorporated into an adsorbent.

However, as the concentration of metal is beyond the ideal value, the active sites on carbon become saturated, the redundant metal cannot be bound and will block the pores in the parent carbon [195], resulting in the decrease of surface area, which will weaken the CO_2 adsorption capacity of MPC. Thus, the loading amount of metal or the ratio of metal impregnated to the parent carbon is a key factor to produce an ideal MPC with appropriate pore size and abundant pores for the adsorption of the CO_2 molecule. It has been verified that the porosity of MPC was inversely proportional to the loading amount of metal ion supplied [191]. Moreover, different kinds of metal show diverse affinity towards the CO_2 molecule [196], so the MPCs with different metals have distinct adsorption performance. For example, the adsorption capacity of CO_2 on metal-impregnated AC followed the order of Fe(III) > Mg(II) > Cu(II) > Ag(I)/AC. The incorporation of Fe and Mg enhanced the bonding with AC because Fe^{3+} and Mg^{2+} are hard acids, while the addition of Ag onto AC weakened the CO_2 adsorption for Ag^{+} is a soft acid.

Apart from the ratio and type of metals, the metal precursor used in the adsorbent preparation also has important effects on the adsorption performance of the resultant MPC. Guo et al. [197] found that the hydromagnesite derived Mg-impregnated MPC exhibited lower CO_2 uptake than that of the organometallic magnesium precursor, because there existed other compounds in hydromagnesite derived MgO, such as SiO_2, CaO, Fe_2O_3 and Al_2O_3, which might block the active sites for CO_2 adsorption [198]. Furthermore, the surface area, crystalline size and the impurities in the adsorbent can influence the adsorption capacity. The hydromagenesite derived MgO-impregnated MPC possessed flake and sheet-like geometry with a uniform microparticle dispersion, while the organometallic magnesium precursor derived MPC had a larger specific surface area and pore volume, smaller crystallite size and nanoparticle dispersion resulting in a better CO_2 adsorption performance. In a word, the amount/ratio and type of metal precursor must be chosen prudently to achieve an ideal CO_2 adsorption capacity for MPC, because they determine the morphology, crystallize size, surface area, pore volume and size, which play crucial roles in attaining the optimal CO_2 adsorption performance.

The adsorption process towards CO_2 onto MPC can be summarized into five sequential phases. Specifically, it consists of these following diffusion and adsorption steps: (1) bulk diffusion during which CO_2 diffuse from concentrated gas phase to the surface of MPC; (2) Film diffusion where CO_2 molecule diffuse from the gas film; (3) Interparticle diffusion where the adsorbed CO_2 molecules diffuse into the pores of MPC; (4) Intraparticle diffusion where the adsorbed CO_2 molecules diffuse into the crystalline grains of MPC; (5) Surface adsorption when CO_2 molecule react or interact with the surface/functional groups of MPC [199]. Generally, the fifth step is very rapid, and the correlated resistance is found to be minimal [199]. The actual CO_2 adsorption onto MPC occurs on the basis of these steps, sometimes parts of the adsorption sequence occur, and sometimes, a combination of these sequences occurs. The adsorption of CO_2 onto MPC also mainly depends on physisorption via van der Waals force with a low heat of adsorption ranging from −25 to −40 kJ/mol, which is comparable to the sublimation heat of MPC [34]. For Ca-modified biochar, the isosteric heat of adsorption for CO_2 ranged from 29 to 33 kJ mol^{-1}, indicating a predominant physisorption mechanism with moderate strength, consistent with its excellent regeneration stability (93% capacity retention after five cycles) [200]. Physisorption is known as an exothermic process with low enthalpy value owing to the weak van der Waals attraction forces. The amount of molecules adsorbed is connected with the topological dimension of carbon pores and the pore volume of MPC [201], while it is inversely proportional to the number of pores filled with the metal oxide. Besides physisorption, chemisorption also plays an important role in the CO_2 adsorption onto MPC. As illustrated in Figure 11, physical adsorption, chemical adsorption and hydrogen bonding synergistically contributed to the adsorption of CO_2 onto Mg-impregnated mesoporous carbons. Liu et al. [187] disclosed the adsorption mechanism of CO_2 on Mg-MPC by FTIR and XPS analyses. Based on the results, they concluded that the high CO_2 adsorption capacity (5.45 mmol/g) cannot be solely ascribed to the surface area; the special functional groups on MPC-MgO also played an important role. According to the XPS spectra before and

after adsorption of CO_2 indicated, the O^{2-} at the edges and corners of the MgO crystal were the main active sites for CO_2 capture.

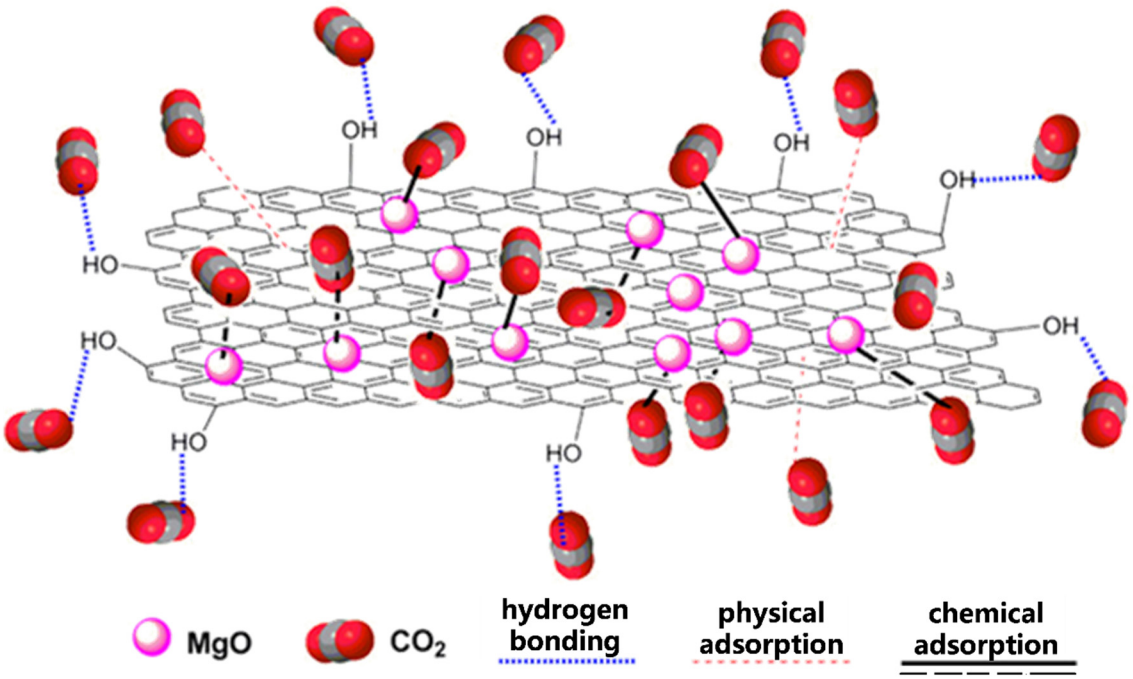

Figure 11. Plausible mechanism of CO_2 adsorption onto magnesium impregnated mesoporous carbon (MPC-MgO) (Reproduced from Ref. [187], with permission from ACS publications).

As displayed in the Figure 12, Azmi et al. [184] proposed the adsorption mechanism of Mg-impregnated hydrochar, offering insights into the interactions governing the phenomenon of enhanced CO_2 adsorption. The process also involves CO_2 binding to the carbon and carbon@MgO surfaces, and the adsorption is a combination of physical and chemical interactions. Nitrogen functional groups act as Lewis bases, forming coordinate covalent bonds with CO_2 molecules. Simultaneously, the MgO contributes to the Lewis acid sites, facilitating chemisorption and the formation of carbonate species on its surface. In addition, hydrogen bonding plays a significant role between the oxygen atoms of CO_2 and nitrogen functional groups. The porous structure of porous carbon boosts the physical adsorption via van der Waals forces. The positively charged sites on MgO and partial charges on CO_2 result in electrostatic attractions, which further contribute to the overall adsorption process, enhancing the adsorption capacity. In summary, the synergistic effects of MgO, nitrogen functionalities and the porous structure of porous carbon create a multifaceted adsorption system. These multiple interactions highlight the complexity of CO_2 adsorption onto this composite adsorbent, along with the hydrogen bonding and electrostatic/diffuse adsorption that play essential roles in the comprehensive adsorption mechanism.

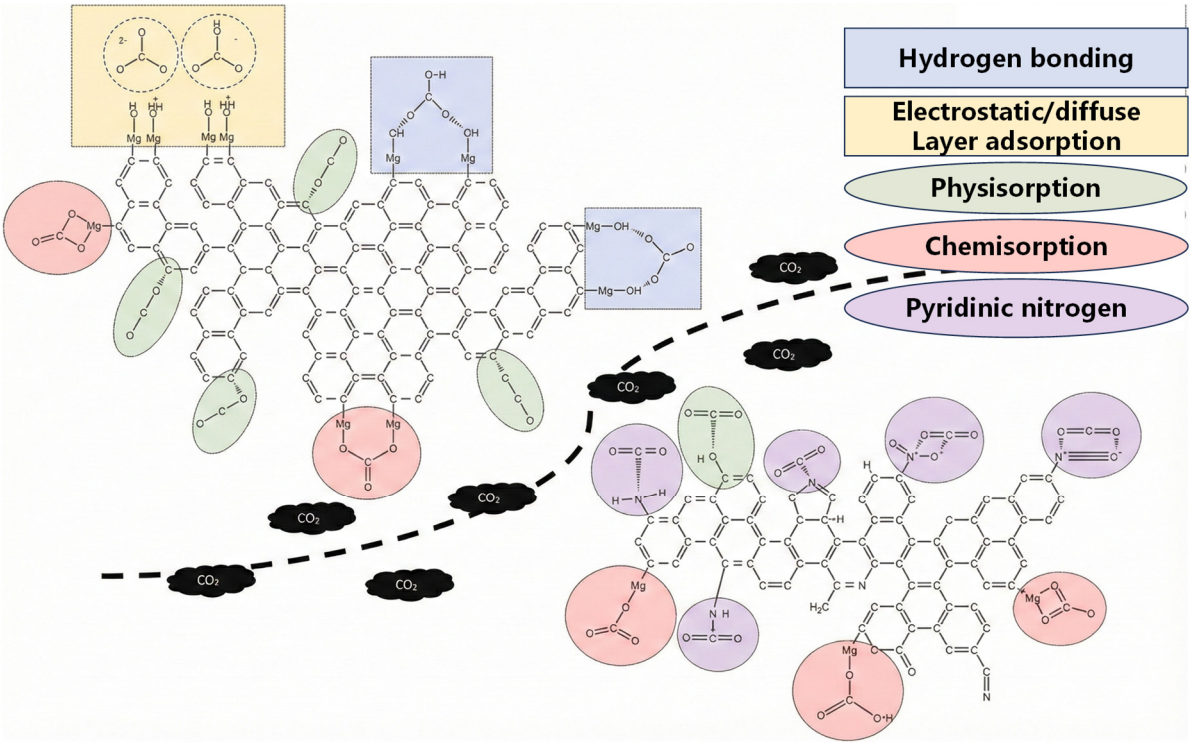

Figure 12. Proposed possible adsorption mechanism of carbon dioxide onto hydrochar impregnated with MgO (Reproduced from Ref. [184], with permission from Elsevier).

4.4. Other Strategies

Recently, an activated carbon based "charged-adsorbent" was developed to capture CO_2 effectively. As displayed in Figure 13, the preparation of charged-adsorbents is on the basis of charging of an electrochemical energy storage device [202], in which the electrolyte ions accumulate in the pores of a conductive porous carbon electrode during charging. After the completion of the charging process, the electrode is removed from the cell and washed/dried to yield a charged-adsorbent material. It is hypothesized that the accumulated ions in the porous electrode can serve as active sites for the adsorption of CO_2. The resulting charged porous carbon can rapidly capture CO_2 from ambient air by means of (bi)carbonate formation, showing enhanced CO_2 uptake at low pressure, and can be regenerated at low temperature of 90–100 °C by direct Joule heating. Given the highly tailorable pore environments and low cost, in which the electrolyte and electrode can easily be adjusted, this charged-adsorbent is expected to have numerous potential applications in separations, catalysis and beyond.

Traditionally, capturing CO_2 by adsorption onto porous carbons mainly depends on the three-dimensional (3D) pores, while two-dimensional (2D) pores in graphene are ideally suited for ambitious high-performance carbon capture. Hsu et al. [203] developed a strategy for improving the carbon capture performance by increasing the binding affinity of CO_2 with the 2D pore. They incorporated pyridinic nitrogen at the pore edges by a simple exposure of ammonia to oxidized single-layer graphene at room temperature. The resultant highly selective 2D pores in graphene led to improved separation performance compared with other membranes for carbon capture. The pyridinic-N-substituted graphene pores can readily adsorb CO_2 even from a very dilute mixture. An attractive combination of CO_2/N_2 selectivity (average of 53) and CO_2 permeance (ca. 10420 GPU) was achieved, which was attributed to the high affinity combined with the 2D nature of the pores.

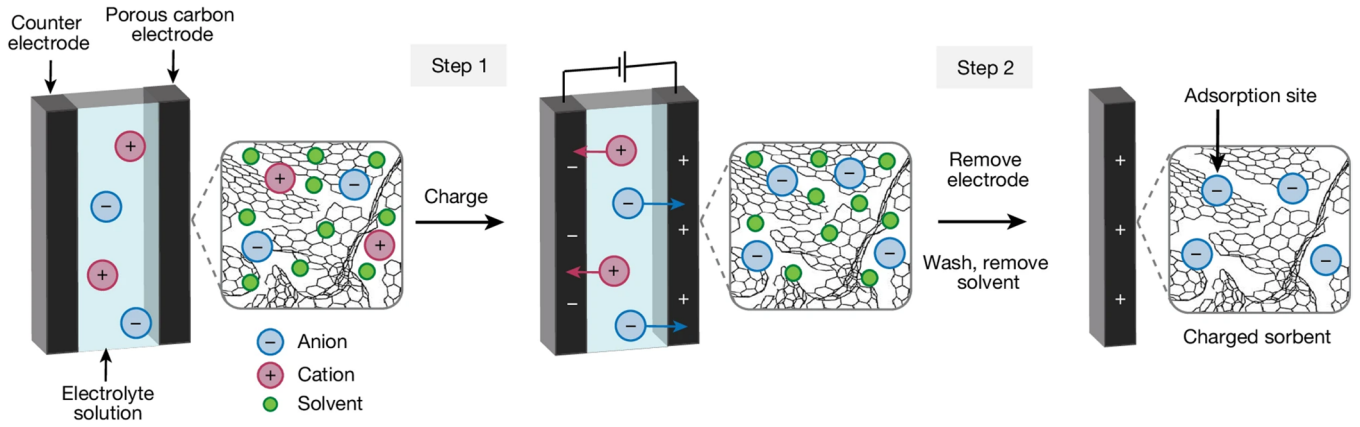

Figure 13. Schematic illustration of the preparation of porous carbon based charged-adsorbents (Reproduced from Ref. [202], with permission from Nature groups).

As we all know, the CO_2 adsorption performance of porous carbon is primarily determined by its texture and surface chemistry, along with the doped heteroatoms and impregnated metal oxides. However, the complicated interplay between the textural and chemical properties of carbon prevents the comprehensive understanding of their respective contributions to CO_2 adsorption capacity and selectivity. Eichler et al. [204] employed a dual cation activation method to control the fine pore structure of carbon independent from its surface N-content. By this method, the surface area can deviate significantly from 2200 to 4500 m^2/g (note: values exceeding ~2630 m^2g^{-1}, the theoretical maximum for both sides of a graphene sheet, may arise from measurement artefacts or model-dependent estimations in highly microporous carbons) at a constant total nitrogen content of 2.3 ± 0.3 at%, or the surface area changed less from 400 to 675 m^2/g at 23.1 ± 0.1at% N derived from nitrogen-rich precursor. From these carbons with variable porosity and constant heteroatom content, not only can the nature of the different adsorption sites be uncovered, but also the fundamental linear free energy exchange relationship can be established accordingly. Their results indicated that selectivity is almost entirely a function of relative porosity for physisorptive carbons, while the surface chemistry plays a negligible role in physisorption of either CO_2 or N_2 at the relevant flue gas conditions. The principal adsorption site is correlated with the narrowest pores that can accommodate a CO_2 molecule (pore width < 0.37 nm).

A comparative summary of the CO_2 adsorption performance for representative porous carbons developed via different strategies is provided in Table 3, highlighting the effectiveness of each approach under specified conditions.

Table 3. Comparison of CO_2 adsorption performance of various modified porous carbon-based adsorbents.

Precursor	Modification Strategy	S_{BET} ($m^2 \cdot g^{-1}$)	Pore Volume ($cm^3 \cdot g^{-1}$)	Adsorption Conditions	CO_2 Uptake ($mmol \cdot g^{-1}$)	Selectivity (CO_2/N_2)	Key Feature	Refs.
Rice husk	KOH activation	1496	0.786	273 K, 1 bar	5.83	9.5	High micropore volume	[41]
Coal	K_2CO_3 activation	1703	0.83	273 K, 1 bar	4.80	N/R	High volumetric capacity	[122]
ZIF-8	N-doped carbon (KCl/NaCl)	1000	0.40	273 K, 1 bar	6.70	39.5	High pyrrolic-N content	[141]
Bamboo shoot shell	N-doping (urea, K_2CO_3)	1985	0.84	273 K, 1 bar	7.52	N/R	Fibrous, worm-like pores	[143]
Oxytetracycline residue	*In-situ* N-doping, KOH	1300	0.55	273 K, 1 bar	6.40	32.0	Waste-derived, *in-situ* N	[142]
Fir sawdust	N, S co-doping	1400	0.60	298 K, 1 bar	3.96	47.0	Secondary activation	[144]

Coconut shell	Molten salt ($NaOH$-Na_2CO_3)	3313	1.67	273 K, 1 bar	6.02	N/R	Ultra-high SSA, N/O co-doping	[109]
Hickory chips	FeOOH impregnation	N/R	N/R	298 K, 1 bar	3.64	N/R	Metal-biochar composite	[189]
Walnut shell	MgO impregnation	292	0.15	298 K, 1 bar	1.86	N/R	Metal oxide enhances chemisorption	[152]

N/R: Not Reported.

Moreover, beyond the initial adsorption capacity, the long-term cyclic stability and efficient regenerability of these modified porous carbons are paramount for practical deployment. For porosity-tuned carbons, physical adsorption is highly reversible, but pore blockage by impurities in real flue gas can gradually degrade performance. Surface modification via heteroatom doping, while enhancing affinity, must ensure the chemical stability of the introduced functional groups (e.g., N-species) over repeated adsorption-regeneration cycles, often involving thermal or pressure swings. Metal impregnation presents more complex challenges, as metal species may sinter, leach, or form stable carbonates, leading to irreversible capacity loss and increased energy demand for regeneration. Therefore, future research on these enhancement strategies must systematically incorporate rigorous cycling tests (e.g., >100 cycles) under realistic conditions, reporting not only capacity retention but also changes in adsorbent structure and kinetics, to truly advance the development of viable adsorbents for industrial CO_2 capture.

Beyond the pursuit of high adsorption capacity and selectivity, the practical deployment of porous carbon adsorbents ultimately hinges on their overall process economics. The cost of adsorbent production is heavily influenced by the choice of precursor (e.g., low-cost biomass *vs*. refined chemicals) and the activation method (e.g., corrosive chemical activation *vs*. greener physical activation). More critically, the energy required for regeneration—often the dominant operational expense—is directly linked to the adsorption mechanism: physisorption-dominated carbons enable low-temperature (e.g., 80–120 °C) or vacuum-driven regeneration, whereas materials enhanced by strong chemisorption (e.g., metal-impregnated carbons) typically demand higher energy input for desorption. Furthermore, the cyclic stability and lifetime of the adsorbent under real flue gas conditions directly amortize its initial cost. Therefore, future research on enhancing CO_2 adsorption must increasingly couple material design with preliminary techno-economic considerations, evaluating not just the "grams of CO_2 captured per gram of adsorbent" but also the "kilojoules required per mole of CO_2 regenerated" and the "cost per ton of CO_2 captured over the adsorbent's lifetime.

5. Conclusions and Future Perspectives

Porous carbons exhibit considerable advantages in CO_2 capture; however, their insufficient adsorption capacity and poor selectivity hinder practical large-scale applications. To address these limitations, numerous modification strategies have been developed. This review systematically summarizes the research progress in porous carbon-based CO_2 adsorption, with a particular focus on strategies for enhancing adsorption performance. Key strategies are comprehensively discussed, including porosity regulation via various methods, surface modification (e.g., heteroatom doping, metal impregnation), and other emerging approaches. Despite significant advancements in this field, further studies are required to improve the adsorption and separation performance of porous carbons, focusing on the following aspects:

(1) Developing efficient pore-formation strategies to fabricate porous carbons with tailored micro-meso-macro porous structures remains highly desirable yet challenging. Traditional physical or chemical activation alone typically yields microporous or micro-mesoporous carbons. Future research should prioritize establishing the relationship between the micro-meso-macro pore ratio and CO_2 mass

transfer/adsorption capacity. As highlighted earlier, adsorption capacity is predominantly determined by micropores—especially ultramicropores (<0.8 nm)—whereas mesopores and macropores govern CO_2 diffusion, adsorption rate, and regenerability. Thus, fabricating porous carbons with optimized micro-meso-macro structures and elucidating the effect of pore ratio on CO_2 capture performance is of great significance.

(2) Greater efforts should be devoted to developing synthetic strategies for heteroatom-doped porous carbons with selective introduction of functional groups that enhance CO_2 adsorption and separation. Heteroatom-derived functionalities exert distinct effects on CO_2 adsorption: for nitrogen doping, only pyridonic and pyridinic N exhibit positive effects, whereas quaternary and oxidized N have negligible or even adverse impacts. Unfortunately, effective methods for doping specific nitrogen-containing groups are lacking, and precise regulation of their distribution, content, and thermal stability remains challenging. Simultaneously, the relationship between nitrogen doping and CO_2 adsorption performance needs to be clarified from both fundamental and application perspectives. Additionally, more research should focus on the preparation, application, and mechanism of porous carbons doped with other heteroatoms (e.g., S, P) for CO_2 adsorption.

(3) It is crucial to develop efficient strategies for fabricating porous carbons with tunable pore structures and optimal surface functionalities. Moreover, understanding the competitive adsorption between CO_2 and flue gas impurities (e.g., H_2O, NO_x, SO_x) is essential for designing high-performance adsorbents. Generally, heteroatom doping (N, S, P, *etc*.) often reduces specific surface area and causes pore collapse, increasing hydrophilicity while decreasing CO_2 adsorption capacity. Operating conditions (temperature, pressure, coexisting gases) also significantly affect CO_2 adsorption during flue gas recycling. Notably, flue gas impurities (dust, SO_2, NO_x) are detrimental to adsorbents and difficult to completely remove; even low concentrations accumulate to significant levels over long-term operation due to the large flow rate and prolonged duration of flue gases, severely degrading adsorption performance. Elucidating the competitive adsorption mechanism between CO_2 and these pollutants is therefore critical for developing porous carbon-based adsorbents with excellent performance in real flue gas environments.

(4) Increased attention should be paid to the preparation and application of metal-impregnated porous carbons (MPCs) for CO_2 adsorption. Recent studies have demonstrated that MPCs are efficient and cost-effective due to their high regenerability; however, they have not been widely adopted in practical CO_2 capture. To promote their large-scale application, future advancements should focus on two aspects: developing novel hybrid MPCs and optimizing regeneration strategies. Comprehensive investigations into the potential of MPCs as alternative CO_2 adsorbents are required, specifically focusing on: (I) optimizing preparation parameters (metal type, loading amount, synthesis techniques) to enhance adsorption performance; (II) selecting suitable carbon sources and fabricating porous carbons with appropriate structures for efficient metal oxide impregnation; (III) developing functionalized hybrid MPCs via compositing with other inorganic/organic nanostructures (e.g., amines, nitrogen-containing compounds); and (IV) clarifying the CO_2-MPC interaction mechanism through combined experimental and theoretical studies.

Statement of the Use of Generative AI and AI-Assisted Technologies in the Writing Process

During the preparation of this manuscript, the authors used Deepseek in order to enhance linguistic quality. After using this tool/service, the authors reviewed and edited the content as needed and take full responsibility for the content of the published article.

Acknowledgments

We express our thanks for funding support from the National Natural Science Foundation of China (No. 52063016, No. 52372048, No. 52202336), the Key Laboratory of Advanced Materials of Ministry of Education (No. Advmat-2421), and the Graduate Innovative Fund of Wuhan Institute of Technology (No. CX2024037).

Author Contributions

Writing—review & editing, Funding, J.W.; Resources, G.Y.; Validation, Investigation, Formal analysis, Funding, L.W.; Investigation, Formal analysis, Funding, B.Z.; Formal analysis, Z.W.; Supervision, Project administration, Z.H.; Investigation, Formal analysis, G.L.; Writing—review & editing, Project administration, Conceptualization, M.W.

Ethics Statement

Not applicable.

Informed Consent Statement

Not applicable.

Data Availability Statement

Relevant information and dates can be made available upon request.

Funding

The work was financially supported by the Fund of National Natural Science Foundation of China (No. 52063016, No. 52372048, No. 52202336), the Fund of Key Laboratory of Advanced Materials of Ministry of Education (No. Advmat-2421), and the Graduate Innovative Fund of Wuhan Institute of Technology (No. CX2025146).

Declaration of Competing Interest

The authors declare that they have no known competing financial interests or personal relationships that could have appeared to influence the work reported in this paper.

References

1. Ghanbari T, Abnisa F, Daud WMAW. A review on production of metal organic frameworks (MOF) for CO_2 adsorption. *Sci. Total Environ.* **2020**, *707*, 135090. DOI:10.1016/j.scitotenv.2019.135090
2. Rong W, Ding M, Wang Y, Kong S, Yao J. Porous biochar with a tubular structure for photothermal CO_2 cycloaddition: One-step doping versus two-step doping. *Sep. Purif. Technol.* **2025**, *353*, 128427. DOI:10.1016/j.seppur.2024.128427
3. Lee G, Ahmed I, Jhung SH. CO_2 adsorption using functionalized metal-organic frameworks under low pressure: Contribution of functional groups, excluding amines, to adsorption. *Chem. Eng. J.* **2024**, *481*, 148440. DOI:10.1016/j.cej.2023.148440
4. Adegoke KA, Oyedotun KO, Ighalo JO, Amaku JF, Olisah C, Adeola AO, et al. Cellulose derivatives and cellulose-metal-organic frameworks for CO_2 adsorption and separation. *J. CO2 Util.* **2022**, *64*, 102163. DOI:10.1016/j.jcou.2022.102163
5. Peters GP, Le Quéré C, Andrew RM, Canadell JG, Friedlingstein P, Ilyina T, et al. Towards real-time verification of CO_2 emissions. *Nat. Clim. Change.* **2017**, *7*, 848–850. DOI:10.1038/s41558-017-0013-9
6. Friedlingstein P, O'sullivan M, Jones MW, Andrew RM, Gregor L, Hauck J, et al. Global carbon budget 2022. *Earth Syst. Sci. Data* **2022**, *14*, 4811–4900. DOI:10.5194/essd-14-4811-2022
7. Rogelj J, Den Elzen M, Höhne N, Fransen T, Fekete H, Winkler H, et al. Paris Agreement climate proposals need a boost to keep warming well below 2 °C. *Nature* **2016**, *534*, 631–639. DOI:10.1038/nature18307

8. Karimi M, Shirzad M, Silva JAC, Rodrigues AE. Biomass/Biochar carbon materials for CO_2 capture and sequestration by cyclic adsorption processes: A review and prospects for future directions. *J. CO_2 Util.* **2022**, *57*, 101890. DOI:10.1016/j.jcou.2022.101890
9. Keshavarz L, Ghaani MR, MacElroy JD, English NJ. A comprehensive review on the application of aerogels in CO_2-adsorption: Materials and characterisation. *Chem. Eng. J.* **2021**, *412*, 128604. DOI:10.1016/j.cej.2021.128604
10. Shen Y. Preparation of renewable porous carbons for CO_2 capture—A review. *Fuel Process. Technol.* **2022**, *236*, 107437. DOI:10.1016/j.fuproc.2022.107437
11. Balasubramanian R, Chowdhury S. Recent advances and progress in the development of graphene-based adsorbents for CO_2 capture. *J. Mater. Chem. A* **2015**, *3*, 21968–21989. DOI:10.1039/c5ta04822b
12. Li J-R, Ma Y, McCarthy MC, Sculley J, Yu J, Jeong H-K, et al. Carbon dioxide capture-related gas adsorption and separation in metal-organic frameworks. *Coord. Chem. Rev.* **2011**, *255*, 1791–1823. DOI:10.1016/j.ccr.2011.02.012
13. Rochelle GT. Amine scrubbing for CO_2 capture. *Science* **2009**, *325*, 1652–1654. DOI:10.1126/science.1176731
14. Zhang Y, Wang S, Feng D, Gao J, Dong L, Zhao Y, et al. Functional biochar synergistic solid/liquid-phase CO_2 capture: A review. *Energy Fuels* **2022**, *36*, 2945–2970. DOI:10.1021/acs.energyfuels.1c04372
15. Fazlollahi F, Saeidi S, Safdari MS, Sarkari M, Klemeš JJ, Baxter LL. Effect of operating conditions on cryogenic carbon dioxide removal. *Energy Technol.* **2017**, *5*, 1588–1598. DOI:10.1002/ente.201600802
16. Creamer AE, Gao B. Carbon-based adsorbents for postcombustion CO_2 capture: A critical review. *Environ. Sci. Technol.* **2016**, *50*, 7276–7289. DOI:10.1021/acs.est.6b00627
17. Karimi M, Rodrigues AE, Silva JA. Designing a simple volumetric apparatus for measuring gas adsorption equilibria and kinetics of sorption. Application and validation for CO_2, CH_4 and N_2 adsorption in binder-free beads of 4A zeolite. *Chem. Eng. J.* **2021**, *425*, 130538. DOI:10.1016/j.cej.2021.130538
18. Zhu X, Li S, Shi Y, Cai N. Recent advances in elevated-temperature pressure swing adsorption for carbon capture and hydrogen production. *Prog. Energy Combust. Sci.* **2019**, *75*, 100784. DOI:10.1016/j.pecs.2019.100784
19. Sreenivasulu B, Sreedhar I, Suresh P, Raghavan KV. Development trends in porous adsorbents for carbon capture. *Environ. Sci. Technol.* **2015**, *49*, 12641–12661. DOI:10.1021/acs.est.5b03149
20. Omodolor IS, Otor HO, Andonegui JA, Allen BJ, Alba-Rubio AC. Dual-function materials for CO_2 capture and conversion: A review. *Ind. Eng. Chem. Res.* **2020**, *59*, 17612–17631. DOI:10.1021/acs.iecr.0c02218
21. Belaissaoui B, Le Moullec Y, Willson D, Favre E. Hybrid membrane cryogenic process for post-combustion CO_2 capture. *J. Membr. Sci.* **2012**, *415*, 424–434. DOI:10.1016/j.memsci.2012.05.029
22. Sun J, Liang C, Tong X, Guo Y, Li W, Zhao C, et al. Evaluation of high-temperature CO_2 capture performance of cellulose-templated CaO-based pellets. *Fuel* **2019**, *239*, 1046–1054. DOI:10.1016/j.fuel.2018.11.123
23. Veneman R, Zhao W, Li Z, Cai N, Brilman DW. Adsorption of CO_2 and H_2O on supported amine sorbents. *Int. J. Greenh. Gas Control.* **2014**, *41*, 268–275. DOI:10.1016/j.ijggc.2015.07.014
24. Karimi M, Silva JAC, Gonçalves CNDP, de Tuesta JLD, Rodrigues AE, Gomes HT. CO_2 capture in chemically and thermally modified activated carbons using breakthrough measurements: experimental and modeling study. *Ind. Eng. Chem. Res.* **2018**, *57*, 11154–11166. DOI: 10.1021/acs.iecr.8b00953
25. Obi D, Onyekuru S, Orga A. Review of recent process developments in the field of carbon dioxide (CO_2) capture from power plants flue gases and the future perspectives. *Int. J. Sustain. Energy* **2024**, *43*, 2317137. DOI:10.1080/14786451.2024.2317137
26. Li Z, Shi K, Zhai L, Wang Z, Wang H, Zhao Y, et al. Constructing multiple sites of metal-organic frameworks for efficient adsorption and selective separation of CO_2. *Sep. Purif. Technol.* **2023**, *307*, 122725. DOI:10.1016/j.seppur.2022.122725
27. Essih S, Vilarrasa-Garcia E, Azevedo DCS, Ballesteros-Plata D, Barroso-Martin I, Infantes-Molina A, et al. Zeolites synthesis from phyllosilicates and their performance for CO_2 adsorption. *Environ. Sci. Pollut. Res.* **2024**, *31*, 37298–37315. DOI:10.1007/s11356-024-33685-0
28. Guo S, Li Y, Wang Y, Wang L, Sun Y, Liu L. Recent advances in biochar-based adsorbents for CO_2 capture. *Carbon Capture Sci. Technol.* **2022**, *4*, 100059. DOI:10.1016/j.ccst.2022.100059
29. Creamer AE, Gao B, Zhang M. Carbon dioxide capture using biochar produced from sugarcane bagasse and hickory wood. *Chem. Eng. J.* **2014**, *249*, 174–179. DOI:10.1016/j.cej.2014.03.105
30. Wu R, Bao A. Preparation of cellulose carbon material from cow dung and its CO_2 adsorption performance. *J. CO2 Util.* **2023**, *68*, 102377. DOI:10.1016/j.jcou.2022.102377
31. Hou Y, Chen Y, He X, Wang F, Cai Q, Shen B. Insights into the adsorption of CO_2, SO_2 and NO_x in flue gas by carbon materials: A critical review. *Chem. Eng. J.* **2024**, *490*, 151424. DOI:10.1016/j.cej.2024.151424
32. Di H, Zhang T, Ma H, Zhang G, Li K, Han J, et al. Biomass tar modified biochar with enhanced micropores and oxygen content for high efficiency CO_2 capture. *Sep. Purif. Technol.* **2025**, *378*, 134678. DOI:10.1016/j.seppur.2025.134678

33. Raganati F, Miccio F, Ammendola P. Adsorption of carbon dioxide for post-combustion capture: A review. *Energy Fuels* **2021**, *35*, 12845–12868. DOI:10.1021/acs.energyfuels.1c01618
34. Alfe M, Policicchio A, Lisi L, Gargiulo V. Solid sorbents for CO_2 and CH_4 adsorption: The effect of metal organic framework hybridization with graphene-like layers on the gas sorption capacities at high pressure. *Renew. Sustain. Energy Rev.* **2021**, *141*, 110816. DOI:10.1016/j.rser.2021.110816
35. Qiu T, Cao W, Xie K, Ahmad F, Zhao W, Mostafa E, et al. CO_2 capture performances of H_3PO_4/KOH activated microwave pyrolyzed porous biochar. *Sustain. Carbon Mater.* **2025**, *1*, e004. DOI:10.48130/scm-0025-0004
36. Sun J, Li H, Liu Q, Zhong W, Dong W. Recent advances in biomass-derived porous carbons for post-combustion CO_2 capture: From preparation and adsorption mechanisms to applications. *Chem. Eng. J.* **2025**, *520*, 165890. DOI:10.1016/j.cej.2025.165890
37. Harris PJF. Structural models of non-graphitising carbon: A brief history. *C* **2025**, *11*, 78. DOI:10.3390/c11040078
38. Whiffen DH. *Manual of Symbols and Terminology for Physicochemical Quantities and Units*; Elsevier: Amsterdam, The Netherlands, 2013.
39. Yang RT. *Adsorbents: Fundamentals and Applications*; John Wiley & Sons: Hoboken, NJ, USA, 2003.
40. Zhang J, Li Q, Zhang J, Liu H, Wang H, Zhang J. Enhanced CO_2 absorption in amine-based carbon capture aided by coconut shell-derived nitrogen-doped biochar. *Sep. Purif. Technol.* **2025**, *353*, 128451. DOI:10.1016/j.seppur.2024.128451
41. Sakib S, Woo HK, Karua P, Salauddin M, Zheng W, Cai L, et al. Sustainable production of nitrogen-doped hierarchical porous carbons from fruit peel wastes for high-performance CO_2 capture. *Sep. Purif. Technol.* **2026**, *380*, 135501. DOI:10.1016/j.seppur.2025.135501
42. He S, Chen G, Xiao H, Shi G, Ruan C, Ma Y, et al. Facile preparation of N-doped activated carbon produced from rice husk for CO_2 capture. *J. Colloid Interface Sci.* **2021**, *582*, 90–101. DOI:10.1016/j.jcis.2020.08.021
43. Wei H, Deng S, Hu B, Chen Z, Wang B, Huang J, et al. Granular bamboo-derived activated carbon for high CO_2 adsorption: the dominant role of narrow micropores. *ChemSusChem* **2012**, *5*, 2354–2360. DOI:10.1002/cssc.201200570
44. Silvestre-Albero J, Wahby A, Sepúlveda-Escribano A, Martínez-Escandell M, Kaneko K, Rodríguez-Reinoso F. Ultrahigh CO_2 adsorption capacity on carbon molecular sieves at room temperature. *Chem. Commun.* **2011**, *47*, 6840–6842. DOI:10.1039/c1cc11618e
45. Lu T, Bai J, Demir M, Hu X, Huang J, Wang L. Synthesis of potassium bitartrate-derived porous carbon via a facile and self-activating strategy for CO_2 adsorption application. *Sep. Purif. Technol.* **2022**, *296*, 121368. DOI:10.1016/j.seppur.2022.121368
46. Nazir G, Rehman A, Park S-J. Self-activated, urea modified microporous carbon cryogels for high-performance CO_2 capture and separation. *Carbon* **2022**, *192*, 14–29. DOI:10.1016/j.carbon.2022.02.040
47. Xing L-A, Yang F, Zhong X, Liu Y, Lu H, Guo Z, et al. Ultra-microporous cotton fiber-derived activated carbon by a facile one-step chemical activation strategy for efficient CO_2 adsorption. *Sep. Purif. Technol.* **2023**, *324*, 124470. DOI:10.1016/j.seppur.2023.124470
48. Kwiatkowski M, Kalderis D, Tono W, Tsubota T. Numerical analysis of the micropore structure of activated carbons focusing on optimum CO_2 adsorption. *J. CO_2 Util.* **2022**, *60*, 101996. DOI:10.1016/j.jcou.2022.101996
49. Singh G, Lakhi KS, Sil S, Bhosale SV, Kim I, Albahily K, et al. Biomass derived porous carbon for CO_2 capture. *Carbon* **2019**, *148*, 164–186. DOI:10.1016/j.carbon.2019.03.050
50. Chao C, Deng Y, Dewil R, Baeyens J, Fan X. Post-combustion carbon capture. *Renew. Sustain. Energy Rev.* **2021**, *138*, 110490. DOI:10.1016/j.rser.2020.110490
51. Zhai J, Wang Z, Ouyang J, Xue B, Liu C, Xiao R. Glucose-driven synthesis of N-doped porous carbon from sludge for CO_2 removal in biomass syngas. *Chem. Eng. J.* **2025**, *512*, 162722. DOI:10.1016/j.cej.2025.162722
52. Zeng L, Zeng S, Liu P, Li H, Chen W, Li K. Unveiling the role of pentagonal topological defects in lignocellulose-derived self-assembled N-O co-doped micro-mesoporous biochar for enhanced CO_2 adsorption. *Carbon Capture Sci. Technol.* **2025**, *15*, 100404. DOI:10.1016/j.ccst.2025.100404
53. Tang Z, Zhu J, Zhao Z, Dong H, Du Q, Feng D, et al. Synergistic enhancement of CO_2 adsorption performance of porous biochar by N/O heteroatoms and pore structure: experiment and DFT simulation. *J. Environ. Chem. Eng.* **2025**, *13*, 120149. DOI:10.1016/j.jece.2025.120149
54. Yin Q, Gao Y, Wang R, Zhu X, Gao X, Zhao Z, et al. Influence of Fe-N co-doping on biochar on the adsorption of CO_2. *Chem. Eng. Sci.* **2026**, *320*, 122702. DOI:10.1016/j.ces.2025.122702
55. Barber PS, Griggs CS, Gurau G, Liu Z, Li S, Li Z, et al. Coagulation of chitin and cellulose from 1-ethyl-3-methylimidazolium acetate ionic-liquid solutions using carbon dioxide. *Angew. Chem. Int. Ed.* **2013**, *52*, 12350–12353. DOI:10.1002/ange.201304604
56. Shao J, Wang Y, Che M, Xiao Q, Demir M, Al Mesfer MK, et al. N, S Co-doped porous carbons from coconut shell for

selective CO_2 adsorption. *J. Energy Inst.* **2025**, *123*, 102273. DOI:10.1016/j.joei.2025.102273
57. Kolle JM, Fayaz M, Sayari A. Understanding the effect of water on CO_2 adsorption. *Chem. Rev.* **2021**, *121*, 7280–7345. DOI:10.1021/acs.chemrev.0c00762
58. Li YY, Han KK, Lin WG, Wan MM, Wang Y, Zhu JH. Fabrication of a new MgO/C sorbent for CO_2 capture at elevated temperature. *J. Mater. Chem. A* **2013**, *1*, 12919–12925. DOI:10.1039/c3ta12261a
59. Zhang H, Goeppert A, Olah GA, Prakash GS. Remarkable effect of moisture on the CO_2 adsorption of nano-silica supported linear and branched polyethylenimine. *J. CO_2 Util.* **2017**, *19*, 91–99. DOI:10.1016/j.jcou.2017.03.008
60. Guo B, Wang Y, Shen X, Qiao X, Jia L, Xiang J, et al. Study on CO_2 capture characteristics and kinetics of modified potassium-based adsorbents. *Materials* **2020**, *13*, 877. DOI:10.3390/ma13040877
61. Akpasi SO, Isa YM. Effect of operating variables on CO_2 adsorption capacity of activated carbon, kaolinite, and activated carbon–Kaolinite composite adsorbent. *Water-Energy Nexus* **2022**, *5*, 21–28. DOI:10.1016/j.wen.2022.08.001
62. Luo J, Liu B, Shi R, Guo Y, Feng Q, Liu Z, et al. The effects of nitrogen functional groups and narrow micropore sizes on CO_2 adsorption onto N-doped biomass-based porous carbon under different pressure. *Microporous Mesoporous Mater.* **2021**, *327*, 111404. DOI:10.1016/j.micromeso.2021.111404
63. Wang Q, Tay HH, Zhong Z, Luo J, Borgna A. Synthesis of high-temperature CO_2 adsorbents from organo-layered double hydroxides with markedly improved CO_2 capture capacity. *Energy Environ. Sci.* **2012**, *5*, 7526–7530. DOI:10.1039/c2ee21409a
64. Gao Y, Zhang Z, Wu J, Yi X, Zheng A, Umar A, et al. Comprehensive investigation of CO_2 adsorption on Mg–Al–CO_3 LDH-derived mixed metal oxides. *J. Mater. Chem. A* **2013**, *1*, 12782–12790. DOI:10.1039/c3ta13039h
65. Ramírez-Moreno MJ, Romero-Ibarra IC, Hernández-Pérez M, Pfeiffer H. CO_2 adsorption at elevated pressure and temperature on Mg–Al layered double hydroxide. *Ind. Eng. Chem. Res.* **2014**, *53*, 8087–8094. DOI:10.1021/ie5010515
66. Kong Y, Shen X, Fan M, Yang M, Cui S. Dynamic capture of low-concentration CO_2 on amine hybrid silsesquioxane aerogel. *Chem. Eng. J.* **2016**, *283*, 1059–1068. DOI:10.1016/j.cej.2015.08.034
67. Baraka F, Labidi J. The emergence of nanocellulose aerogels in CO_2 adsorption. *Sci. Total Environ.* **2023**, *912*, 169093. DOI:10.1016/j.scitotenv.2023.169093
68. Siegelman RL, Milner PJ, Kim EJ, Weston SC, Long JR. Challenges and opportunities for adsorption-based CO_2 capture from natural gas combined cycle emissions. *Energy Environ. Sci.* **2019**, *12*, 2161–2173. DOI:10.1039/c9ee00505f
69. Long Y, Tian H, Lee C-H, Li H, Zeng Z, Yang Z, et al. Competitive adsorption of H_2O and CO_2 on nitrogen-doped biochar with rich-oxygen functional groups. *Sep. Purif. Technol.* **2025**, *359*, 130476. DOI:10.1016/j.seppur.2024.130476
70. Li G, Xiao P, Zhang J, Webley PA, Xu D. The role of water on postcombustion CO_2 capture by vacuum swing adsorption: Bed layering and purge to feed ratio. *AlChE J.* **2014**, *60*, 673–689. DOI:10.1002/aic.14281
71. Zhang J, Xiao P, Li G, Webley PA. Effect of flue gas impurities on CO_2 capture performance from flue gas at coal-fired power stations by vacuum swing adsorption. *Energy Procedia.* **2009**, *1*, 1115–1122. DOI:10.1016/j.egypro.2009.01.147
72. Plaza MG, González AS, Rubiera F, Pevida C. Water vapour adsorption by a coffee-based microporous carbon: Effect on CO_2 capture. *J. Chem. Technol. Biotechnol.* **2015**, *90*, 1592–1600. DOI:10.1002/jctb.4636
73. Xu D, Xiao P, Zhang J, Li G, Xiao G, Webley PA, et al. Effects of water vapour on CO_2 capture with vacuum swing adsorption using activated carbon. *Chem. Eng. J.* **2013**, *230*, 64–72. DOI:10.1016/j.cej.2013.06.080
74. Wahby A, Silvestre-Albero J, Sepúlveda-Escribano A, Rodríguez-Reinoso F. CO_2 adsorption on carbon molecular sieves. *Microporous Mesoporous Mater.* **2012**, *164*, 280–287. DOI:10.1016/j.micromeso.2012.06.034
75. Cossarutto L, Zimny T, Kaczmarczyk J, Siemieniewska T, Bimer J, Weber J. Transport and sorption of water vapour in activated carbons. *Carbon* **2001**, *39*, 2339–2346. DOI:10.1016/s0008-6223(01)00065-3
76. Keller JU, Staudt R. *Gas Adsorption Equilibria: Experimental Methods and Adsorptive Isotherms*; Springer: New York, NY, USA, 2005.
77. Do D, Do H. A model for water adsorption in activated carbon. *Carbon* **2000**, *38*, 767–773. DOI:10.1016/S0008-6223(99)00159-1
78. Dubinin M. Water vapor adsorption and the microporous structures of carbonaceous adsorbents. *Carbon* **1980**, *18*, 355–364. DOI:10.1016/0008-6223(80)90007-X
79. Barton SS, Evans MJ, MacDonald JA. The adsorption of water vapor by porous carbon. *Carbon* **1991**, *29*, 1099–1105. DOI:10.1016/0008-6223(91)90026-F
80. Müller EA, Rull LF, Vega LF, Gubbins KE. Adsorption of water on activated carbons: a molecular simulation study. *J. Phys. Chem.* **1996**, *100*, 1189–1196. DOI:10.1021/jp952233w
81. Durán I, Rubiera F, Pevida C. Separation of CO_2 in a solid waste management incineration facility using activated carbon derived from pine sawdust. *Energies* **2017**, *10*, 827. DOI:10.3390/en10060827
82. Younas M, Leong LK, Mohamed AR, Sethupathi S. CO_2 adsorption by modified palm shell activated carbon (PSAC) via

chemical and physical activation and metal impregnation. *Chem. Eng. Commun.* **2016**, *203*, 1455–1463. DOI:10.1080/00986445.2016.1201660

83. Gray M, Johnson MG, Dragila MI, Kleber M. Water uptake in biochars: The roles of porosity and hydrophobicity. *Biomass Bioenergy* **2014**, *61*, 196–205. DOI:10.1016/j.biombioe.2013.12.010
84. Kinney T, Masiello C, Dugan B, Hockaday W, Dean M, Zygourakis K, et al. Hydrologic properties of biochars produced at different temperatures. *Biomass Bioenergy* **2012**, *41*, 34–43. DOI:10.1016/j.biombioe.2012.01.033
85. Kameyama K, Miyamoto T, Iwata Y. The preliminary study of water-retention related properties of biochar produced from various feedstock at different pyrolysis temperatures. *Materials* **2019**, *12*, 1732. DOI:10.3390/ma12111732
86. Ahmad M, Lee SS, Dou X, Mohan D, Sung J-K, Yang JE, et al. Effects of pyrolysis temperature on soybean stover-and peanut shell-derived biochar properties and TCE adsorption in water. *Bioresour. Technol.* **2012**, *118*, 536–544. DOI:10.1016/j.biortech.2012.05.042
87. Fang Q, Chen B, Lin Y, Guan Y. Aromatic and hydrophobic surfaces of wood-derived biochar enhance perchlorate adsorption via hydrogen bonding to oxygen-containing organic groups. *Environ. Sci. Technol.* **2014**, *48*, 279–288. DOI:10.1021/es403711y
88. Ahmad M, Rajapaksha AU, Lim JE, Zhang M, Bolan N, Mohan D, et al. Biochar as a sorbent for contaminant management in soil and water: A review. *Chemosphere* **2014**, *99*, 19–33. DOI:10.1016/j.chemosphere.2013.10.071
89. Sun Y, Wang Y, Zhang Y, Zhou Y, Zhou L. CO_2 sorption in activated carbon in the presence of water. *Chem. Phys. Lett.* **2007**, *437*, 14–16. DOI:10.1016/j.cplett.2007.02.008
90. Shi S, Ochedi FO, Yu J, Liu Y. Porous biochars derived from microalgae pyrolysis for CO_2 adsorption. *Energy Fuels* **2021**, *35*, 7646–7656. DOI:10.1021/acs.energyfuels.0c04091
91. Igalavithana AD, Choi SW, Shang J, Hanif A, Dissanayake PD, Tsang DC, et al. Carbon dioxide capture in biochar produced from pine sawdust and paper mill sludge: Effect of porous structure and surface chemistry. *Sci. Total Environ.* **2020**, *739*, 139845. DOI:10.1016/j.scitotenv.2020.139845
92. Liu S-H, Huang Y-Y. Valorization of coffee grounds to biochar-derived adsorbents for CO_2 adsorption. *J. Cleaner Prod.* **2018**, *175*, 354–360. DOI:10.1016/j.jclepro.2017.12.076
93. Tefera DT, Hashisho Z, Philips JH, Anderson JE, Nichols M. Modeling competitive adsorption of mixtures of volatile organic compounds in a fixed-bed of beaded activated carbon. *Environ. Sci. Technol.* **2014**, *48*, 5108–5117. DOI:10.1021/es404667f
94. Hu J, Liu Y, Liu J, Gu C. Effects of water vapor and trace gas impurities in flue gas on CO_2 capture in zeolitic imidazolate frameworks: The significant role of functional groups. *Fuel* **2017**, *200*, 244–251. DOI:10.1016/j.fuel.2017.03.079
95. Zhang W, Rabiei S, Bagreev A, Zhuang M, Rasouli F. Study of NO adsorption on activated carbons. *Appl. Catal. B* **2008**, *83*, 63–71. DOI:10.1016/j.apcatb.2008.02.003
96. Chen J, Cao F, Chen S, Ni M, Gao X, Cen K. Adsorption kinetics of NO on ordered mesoporous carbon (OMC) and cerium-containing OMC (Ce-OMC). *Appl. Surf. Sci.* **2014**, *317*, 26–34. DOI:10.1016/j.apsusc.2014.08.067
97. Sun F, Gao J, Zhu Y, Chen G, Wu S, Qin Y. Adsorption of SO_2 by typical carbonaceous material: A comparative study of carbon nanotubes and activated carbons. *Adsorption* **2013**, *19*, 959–966. DOI:10.1007/s10450-013-9504-9
98. Sethupathi S, Zhang M, Rajapaksha AU, Lee SR, Mohamad Nor N, Mohamed AR, et al. Biochars as potential adsorbers of CH_4, CO_2 and H_2S. *Sustainability* **2017**, *9*, 121. DOI:10.3390/su9010121
99. Zhao W, Guo X, Zhou Z, Wang Z, Han M, Wang X. Preparation and CO_2 adsorption of N-doped biochar and effect of acetone on its adsorption performance. *J. Environ. Manag.* **2025**, *389*, 126041. DOI:10.1016/j.jenvman.2025.126041
100. Wang Y, Hu X, Hao J, Ma R, Guo Q, Gao H, et al. Nitrogen and oxygen codoped porous carbon with superior CO_2 adsorption performance: A combined experimental and DFT calculation study. *Ind. Eng. Chem. Res.* **2019**, *58*, 13390–13400. DOI:10.1021/acs.iecr.9b01454
101. Yi H, Zuo Y, Liu H, Tang X, Zhao S, Wang Z, et al. Simultaneous removal of SO_2, NO, and CO_2 on metal-modified coconut shell activated carbon. *Water Air Soil Pollut.* **2014**, *225*, 1965. DOI:10.1007/s11270-014-1965-2
102. Deng S, Wei H, Chen T, Wang B, Huang J, Yu G. Superior CO_2 adsorption on pine nut shell-derived activated carbons and the effective micropores at different temperatures. *Chem. Eng. J.* **2014**, *253*, 46–54. DOI:10.1016/j.cej.2014.04.115
103. Abbaspour N, Jordan C, Tondl G, Wąsik P, Gholizadeh T, Tomasetig D, et al. Activated biochars from heavy metal-contaminated biomass for CO_2 capture: Adsorption performance and dominant mechanisms. *J. CO_2 Util.* **2025**, *101*, 103217. DOI:10.1016/j.jcou.2025.103217
104. Rashidi NA, Yusup S. An overview of activated carbons utilization for the post-combustion carbon dioxide capture. *J. CO2 Util.* **2016**, *13*, 1–16. DOI:10.1016/j.jcou.2015.11.002
105. Jagiello J, Kenvin J, Celzard A, Fierro V. Enhanced resolution of ultra micropore size determination of biochars and activated carbons by dual gas analysis using N_2 and CO_2 with 2D-NLDFT adsorption models. *Carbon* **2019**, *144*, 206–215.

DOI:10.1016/j.carbon.2018.12.028
106. Sun Y, Zhao J, Wang J, Tang N, Zhao R, Zhang D, et al. Sulfur-doped millimeter-sized microporous activated carbon spheres derived from sulfonated poly (styrene–divinylbenzene) for CO_2 capture. *J. Phys. Chem. C* **2017**, *121*, 10000–10009. DOI:10.1021/acs.jpcc.7b02195
107. Singh G, Lee J, Karakoti A, Bahadur R, Yi J, Zhao D, et al. Emerging trends in porous materials for CO_2 capture and conversion. *Chem. Soc. Rev.* **2020**, *49*, 4360–4404. DOI:10.1039/d0cs00075b
108. Goetz V, Pupier O, Guillot A. Carbon dioxide-methane mixture adsorption on activated carbon. *Adsorption* **2006**, *12*, 55–63. DOI:10.1007/s10450-006-0138-z
109. Hu Z, Lei L, Li Y, Ni Y. Chromium adsorption on high-performance activated carbons from aqueous solution. *Sep. Purif. Technol.* **2003**, *31*, 13–18. DOI:10.1016/s1383-5866(02)00149-1
110. Xie T, He J, Xu L-C, Yan T, Pan Q-W, Wang L-W, et al. Preparation of N-doped porous biochar with high CO_2 adsorption performance via one-step molten salt thermal treatment. *Chem. Eng. J.* **2025**, *521*, 166621. DOI:10.1016/j.cej.2025.166621
111. Deng S, Hu B, Chen T, Wang B, Huang J, Wang Y, et al. Activated carbons prepared from peanut shell and sunflower seed shell for high CO_2 adsorption. *Adsorption* **2015**, *21*, 125–133. DOI:10.1007/s10450-015-9655-y
112. Nandi M, Okada K, Dutta A, Bhaumik A, Maruyama J, Derks D, et al. Unprecedented CO_2 uptake over highly porous N-doped activated carbon monoliths prepared by physical activation. *Chem. Commun.* **2012**, *48*, 10283–10285. DOI:10.1039/c2cc35334b
113. Sevilla M, Fuertes AB. Sustainable porous carbons with a superior performance for CO_2 capture. *Energy Environ. Sci.* **2011**, *4*, 1765–1771. DOI:10.1039/c0ee00784f
114. Coromina HM, Walsh DA, Mokaya R. Biomass-derived activated carbon with simultaneously enhanced CO_2 uptake for both pre and post combustion capture applications. *J. Mater. Chem. A* **2016**, *4*, 280–289. DOI:10.1039/c5ta09202g
115. Liu C, Wang J, Zhang S, Wei C, Cao L, Zhou Y, et al. Ultramicropore-rich N-doped porous biochar from discarded cigarette butts for efficient CO_2 capture with ultra-high adsorption capacity and selectivity. *Sep. Purif. Technol.* **2025**, *358*, 130205. DOI:10.1016/j.seppur.2024.130205
116. Li J, Michalkiewicz B, Min J, Ma C, Chen X, Gong J, et al. Selective preparation of biomass-derived porous carbon with controllable pore sizes toward highly efficient CO_2 capture. *Chem. Eng. J.* **2019**, *360*, 250–259. DOI:10.1016/j.cej.2018.11.204
117. Everett DH, Powl JC. Adsorption in slit-like and cylindrical micropores in the henry's law region. A model for the microporosity of carbons. *J. Chem. Soc. Faraday Trans. 1 Phys. Chem. Condens. Phases* **1976**, *72*, 619–636. DOI:10.1039/f19767200619
118. Li D, Zhou J, Wang Y, Tian Y, Wei L, Zhang Z, et al. Effects of activation temperature on densities and volumetric CO_2 adsorption performance of alkali-activated carbons. *Fuel* **2019**, *238*, 232–239. DOI:10.1016/j.fuel.2018.10.122
119. Liu J, Liu X, Sun Y, Sun C, Liu H, Stevens LA, et al. High density and super ultra-microporous-activated carbon macrospheres with high volumetric capacity for CO_2 capture. *Adv. Sustain. Syst.* **2018**, *2*, 1700115. DOI:10.1002/adsu.201700115
120. Haffner-Staton E, Balahmar N, Mokaya R. High yield and high packing density porous carbon for unprecedented CO_2 capture from the first attempt at activation of air-carbonized biomass. *J. Mater. Chem. A* **2016**, *4*, 13324–13335. DOI:10.1039/c6ta06407h
121. Guo L, Yang J, Hu G, Hu X, Wang L, Dong Y, et al. Role of hydrogen peroxide preoxidizing on CO_2 adsorption of nitrogen-doped carbons produced from coconut shell. *ACS Sustain. Chem. Eng.* **2016**, *4*, 2806–2813. DOI:10.1021/acssuschemeng.6b00327
122. Fan Z, Cheng Z, Feng J, Xie Z, Liu Y, Wang Y. Ultrahigh volumetric performance of a free-standing compact N-doped holey graphene/PANI slice for supercapacitors. *J. Mater. Chem. A* **2017**, *5*, 16689–16701. DOI:10.1039/c7ta04384h
123. Qie Z, Wang L, Sun F, Xiang H, Wang H, Gao J, et al. Tuning porosity of coal-derived activated carbons for CO_2 adsorption. *Front. Chem. Sci. Eng.* **2022**, *16*, 1345–1354. DOI:10.1007/s11705-022-2155-1
124. Ahmadpour A, Do D. The preparation of active carbons from coal by chemical and physical activation. *Carbon* **1996**, *34*, 471–479. DOI:10.1016/0008-6223(95)00204-9
125. Rehman A, Park S-J. Comparative study of activation methods to design nitrogen-doped ultra-microporous carbons as efficient contenders for CO_2 capture. *Chem. Eng. J.* **2018**, *352*, 539–548. DOI:10.1016/j.cej.2018.07.046
126. Li D, Yang J, Zhao Y, Yuan H, Chen Y. Ultra-highly porous carbon from wasted soybean residue with tailored porosity and doped structure as renewable multi-purpose absorbent for efficient CO_2, toluene and water vapor capture. *J. Cleaner Prod.* **2022**, *337*, 130283. DOI:10.1016/j.jclepro.2021.130283
127. Chen J, Lin J, Luo J, Tian Z, Zhang J, Sun S, et al. Enhanced CO_2 capture performance of N, S co-doped biochar prepared by microwave pyrolysis: Synergistic modulation of microporous structure and functional groups. *Fuel* **2025**, *379*, 132987.

DOI:10.1016/j.fuel.2024.132987
128. Wang L, Sun F, Hao F, Qu Z, Gao J, Liu M, et al. A green trace K_2CO_3 induced catalytic activation strategy for developing coal-converted activated carbon as advanced candidate for CO_2 adsorption and supercapacitors. *Chem. Eng. J.* **2020**, *383*, 123205. DOI:10.1016/j.cej.2019.123205
129. Yuan H, Chen J, Li D, Chen H, Chen Y. 5 Ultramicropore-rich renewable porous carbon from biomass tar with excellent adsorption capacity and selectivity for CO_2 capture. *Chem. Eng. J.* **2019**, *373*, 171–178. DOI:10.1016/j.cej.2019.04.206
130. Saha D, Kienbaum MJ. Role of oxygen, nitrogen and sulfur functionalities on the surface of nanoporous carbons in CO_2 adsorption: A critical review. *Microporous Mesoporous Mater.* **2019**, *287*, 29–55. DOI:10.1016/j.micromeso.2019.05.051
131. Saha D, Van Bramer SE, Orkoulas G, Ho H-C, Chen J, Henley DK. CO_2 capture in lignin-derived and nitrogen-doped hierarchical porous carbons. *Carbon* **2017**, *121*, 257–266. DOI:10.1016/j.carbon.2017.05.088
132. Sreńscek-Nazzal J, Kiełbasa K. Advances in modification of commercial activated carbon for enhancement of CO_2 capture. *Appl. Surf. Sci.* **2019**, *494*, 137–151. DOI:10.1016/j.apsusc.2019.07.108
133. Yong Z, Mata V, Rodrigues AE. Adsorption of carbon dioxide at high temperature—A review. *Sep. Purif. Technol.* **2002**, *26*, 195–205. DOI:10.1016/s1383-5866(01)00165-4
134. Sun S, Yin Z, Cong B, Hong W, Zhou X, Wang Y, et al. Crystalline carbon modified hierarchical porous iron and nitrogen co-doped carbon for efficient electrocatalytic oxygen reduction. *J. Colloid Interface Sci.* **2021**, *594*, 864–873. DOI:10.1016/j.jcis.2021.03.068
135. Wang J, Yin Y, Liu X, Liu Y, Xiao Q, Zhao L, et al. Potassium metaborate-activated boron-doped porous carbons for selective CO_2 adsorption. *Sep. Purif. Technol.* **2025**, *376*, 134079. DOI:10.1016/j.seppur.2025.134079
136. Ma X, Li L, Zeng Z, Chen R, Wang C, Zhou K, et al. Experimental and theoretical demonstration of the relative effects of O-doping and N-doping in porous carbons for CO_2 capture. *Appl. Surf. Sci.* **2019**, *481*, 1139–1147. DOI:10.1016/j.apsusc.2019.03.162
137. Li L, Wang X-F, Zhong J-J, Qian X, Song S-L, Zhang Y-G, et al. Nitrogen-enriched porous polyacrylonitrile-based carbon fibers for CO_2 capture. *Ind. Eng. Chem. Res.* **2018**, *57*, 11608–11616. DOI:10.1021/acs.iecr.8b01836
138. Kumar KV, Preuss K, Lu L, Guo ZX, Titirici MM. Effect of nitrogen doping on the CO_2 adsorption behavior in nanoporous carbon structures: A molecular simulation study. *J. Phys. Chem. C* **2015**, *119*, 22310–22321. DOI:10.1021/acs.jpcc.5b06017
139. Xiao J, Yuan X, Zhang TC, Ouyang L, Yuan S. Nitrogen-doped porous carbon for excellent CO_2 capture: A novel method for preparation and performance evaluation. *Sep. Purif. Technol.* **2022**, *298*, 121602. DOI:10.1016/j.seppur.2022.121602
140. Pietrzak R. XPS study and physico-chemical properties of nitrogen-enriched microporous activated carbon from high volatile bituminous coal. *Fuel* **2009**, *88*, 1871–1877. DOI:10.1016/j.fuel.2009.04.017
141. Nazir G, Rehman A, Ikram M, Aslam M, Zhang TC, Khalid A, et al. Facile synthesis of inherently nitrogen-doped PAN-derived microporous carbons activated with $NaNH_2$ for selective CO_2 adsorption and separation. *Chem. Eng. J.* **2024**, *497*, 154704. DOI:10.1016/j.cej.2024.154704
142. Wang Y, Suo Y, Xu Y, Zhang Z. Enhancing CO_2 adsorption performance of porous nitrogen-doped carbon materials derived from ZIFs: Insights into pore structure and surface chemistry. *Sep. Purif. Technol.* **2024**, *335*, 126117. DOI:10.1016/j.seppur.2023.126117
143. Liu P, Qin S, Wang J, Zhang S, Tian Y, Zhang F, et al. Effective CO_2 capture by *in-situ* nitrogen-doped nanoporous carbon derived from waste antibiotic fermentation residues. *Environ. Pollut.* **2023**, *333*, 121972. DOI:10.1016/j.envpol.2023.121972
144. Wu W, Wu C, Liu J, Yan H, Zhang G, Li G, et al. Nitrogen-doped porous carbon through K_2CO_3-activated bamboo shoot shell for an efficient CO_2 adsorption. *Fuel* **2024**, *363*, 130937. DOI:10.1016/j.fuel.2024.130937
145. Zhang W, Li K, Liu B, Xu W, Sun K, Yue Y. Heteroatom-doped porous activated carbon from fir sawdust: Tunable pore structures for efficient CO_2 and tetracycline adsorption. *Chem. Eng. Sci.* **2026**, *321*, 122886. DOI:10.1016/j.ces.2025.122886
146. Montes-Morán M, Suárez D, Menéndez J, Fuente E. On the nature of basic sites on carbon surfaces: an overview. *Carbon* **2004**, *42*, 1219–1225. DOI:10.1016/j.carbon.2004.01.023
147. Boehm HP. Surface oxides on carbon and their analysis: A critical assessment. *Carbon* **2002**, *40*, 145–149. DOI:10.1016/s0008-6223(01)00165-8
148. Voll M, Boehm H. Basische Oberflächenoxide auf Kohlenstoff—IV. Chemische Reaktionen zur Identifizierung der Oberflächengruppen. *Carbon* **1971**, *9*, 481–488. DOI:10.1016/0008-6223(71)90028-5
149. Plaza M, Thurecht K, Pevida C, Rubiera F, Pis J, Snape C, et al. Influence of oxidation upon the CO_2 capture performance of a phenolic-resin-derived carbon. *Fuel Process. Technol.* **2013**, *110*, 53–60. DOI:10.1016/j.fuproc.2013.01.011
150. Guo Y, Tan C, Sun J, Li W, Zhang J, Zhao C. Porous activated carbons derived from waste sugarcane bagasse for CO_2

adsorption. *Chem. Eng. J.* **2020**, *381*, 122736. DOI:10.1016/j.cej.2019.122736
151. Rajapaksha AU, Chen SS, Tsang DC, Zhang M, Vithanage M, Mandal S, et al. Engineered/designer biochar for contaminant removal/immobilization from soil and water: Potential and implication of biochar modification. *Chemosphere* **2016**, *148*, 276–291. DOI:10.1016/j.chemosphere.2016.01.043
152. Budinova T, Ekinci E, Yardim F, Grimm A, Björnbom E, Minkova V, et al. Characterization and application of activated carbon produced by H_3PO_4 and water vapor activation. *Fuel Process. Technol.* **2006**, *87*, 899–905. DOI:10.1016/j.fuproc.2006.06.005
153. Lahijani P, Mohammadi M, Mohamed AR. Metal incorporated biochar as a potential adsorbent for high capacity CO_2 capture at ambient condition. *J. CO_2 Util.* **2018**, *26*, 281–293. DOI:10.1016/j.jcou.2018.05.018
154. Kudin KN, Ozbas B, Schniepp HC, Prud'homme RK, Aksay IA, Car R. Raman spectra of graphite oxide and functionalized graphene sheets. *Nano Lett.* **2008**, *8*, 36–41. DOI:10.1021/nl071822y
155. Bai BC, Kim EA, Lee CW, Lee Y-S, Im JS. Effects of surface chemical properties of activated carbon fibers modified by liquid oxidation for CO_2 adsorption. *Appl. Surf. Sci.* **2015**, *353*, 158–164. DOI:10.1016/j.apsusc.2015.06.046
156. Tiwari D, Goel C, Bhunia H, Bajpai PK. Novel nanostructured carbons derived from epoxy resin and their adsorption characteristics for CO_2 capture. *RSC Adv.* **2016**, *6*, 97728–97738. DOI:10.1039/c6ra18291g
157. Babu DJ, Bruns M, Schneider R, Gerthsen D, Schneider JJ. Understanding the influence of N-doping on the CO_2 adsorption characteristics in carbon nanomaterials. *J. Phys. Chem. C* **2017**, *121*, 616–626. DOI:10.1021/acs.jpcc.6b11686
158. Liu Y, Wilcox J. Molecular simulation studies of CO_2 adsorption by carbon model compounds for carbon capture and sequestration applications. *Environ. Sci. Technol.* **2013**, *47*, 95–101. DOI:10.1021/es3012029
159. Kazarian SG, Vincent MF, Bright FV, Liotta CL, Eckert CA. Specific intermolecular interaction of carbon dioxide with polymers. *J. Am. Chem. Soc.* **1996**, *118*, 1729–1736. DOI:10.1021/ja950416q
160. Fuente E, Menéndez J, Suarez D, Montes-Morán M. Basic surface oxides on carbon materials: A global view. *Langmuir* **2003**, *19*, 3505–3511. DOI:10.1021/la026778a
161. Singh G, Lakhi KS, Ramadass K, Kim S, Stockdale D, Vinu A. A combined strategy of acid-assisted polymerization and solid state activation to synthesize functionalized nanoporous activated biocarbons from biomass for CO_2 capture. *Microporous Mesoporous Mater.* **2018**, *271*, 23–32. DOI:10.1016/j.micromeso.2018.05.035
162. Liu Y, Wilcox J. Effects of surface heterogeneity on the adsorption of CO_2 in microporous carbons. *Environ. Sci. Technol.* **2012**, *46*, 1940–1947. DOI:10.1021/es204071g
163. Ma X, Li L, Chen R, Wang C, Li H, Wang S. Heteroatom-doped nanoporous carbon derived from MOF-5 for CO_2 capture. *Appl. Surf. Sci.* **2018**, *435*, 494–502. DOI:10.1016/j.apsusc.2017.11.069
164. Ren W, Saito R, Gao L, Zheng F, Wu Z, Liu B, et al. Edge phonon state of mono-and few-layer graphene nanoribbons observed by surface and interference co-enhanced raman spectroscopy. *Phys. Rev. B Condens. Matter.* **2010**, *81*, 035412. DOI:10.1103/PhysRevB.81.035412
165. Denis PA. Concentration dependence of the band gaps of phosphorus and sulfur doped graphene. *Comput. Mater. Sci.* **2013**, *67*, 203–206. DOI:10.1016/j.commatsci.2012.08.041
166. Su W, Yao L, Ran M, Sun Y, Liu J, Wang X. Adsorption properties of N_2, CH_4, and CO_2 on sulfur-doped microporous carbons. *J. Chem. Eng. Data* **2018**, *63*, 2914–2920. DOI:10.1021/acs.jced.8b00227
167. Kiciński W, Szala M, Bystrzejewski M. Sulfur-doped porous carbons: synthesis and applications. *Carbon* **2014**, *68*, 1–32. DOI:10.1016/j.carbon.2013.11.004
168. Xia Y, Zhu Y, Tang Y. Preparation of sulfur-doped microporous carbons for the storage of hydrogen and carbon dioxide. *Carbon* **2012**, *50*, 5543–5553. DOI:10.1016/j.carbon.2012.07.044
169. Seema H, Kemp KC, Le NH, Park S-W, Chandra V, Lee JW, et al. Highly selective CO_2 capture by S-doped microporous carbon materials. *Carbon* **2014**, *66*, 320–326. DOI:10.1016/j.carbon.2013.09.006
170. Zhu C, Fang Q, Liu R, Dong W, Song S, Shen Y. Insights into the crucial role of electron and spin structures in heteroatom-doped covalent triazine frameworks for removing organic micropollutants. *Environ. Sci. Technol.* **2022**, *56*, 6699–6709. DOI:10.1021/acs.est.2c01781
171. Zhou S, Wang M, Wang J, Xin H, Liu S, Wang Z, et al. Carbon phosphides: promising electric field controllable nanoporous materials for CO_2 capture and separation. *J. Mater. Chem. A* **2020**, *8*, 9970–9980. DOI:10.1039/d0ta03262j
172. Khan AA, Ahmad I, Ahmad R. Influence of electric field on CO_2 removal by P-doped C60-fullerene: A DFT study. *Chem. Phys. Lett.* **2020**, *742*, 137155. DOI:10.1016/j.cplett.2020.137155
173. Luo J, Huang H, Sun S, Ma R. Delicately-controlled nitrogen species in porous biochar via microwave-coordinated phosphorus doping for enhancing CO_2 capture: Active sites tuning and synergistic mechanism analysis. *Sep. Purif. Technol.* **2026**, *382*, 136032. DOI:10.1016/j.seppur.2025.136032
174. Abuelnoor N, AlHajaj A, Khaleel M, Vega LF, Abu-Zahra MRM. Activated carbons from biomass-based sources for CO_2

capture applications. *Chemosphere* **2021**, *282*, 131111. DOI:10.1016/j.chemosphere.2021.131111
175. Chen C-Y, Chang H-W, Kao P-C, Pan J-L, Chang J-S. Biosorption of cadmium by CO_2-fixing microalga scenedesmus obliquus CNW-N. *Bioresour. Technol.* **2012**, *105*, 74–80. DOI:10.1016/j.biortech.2011.11.124
176. Creamer AE, Gao B, Wang S. Carbon dioxide capture using various metal oxyhydroxide–biochar composites. *Chem. Eng. J.* **2016**, *283*, 826–832. DOI:10.1016/j.cej.2015.08.037
177. Liu J, Jiang J, Meng Y, Aihemaiti A, Xu Y, Xiang H, et al. Preparation, environmental application and prospect of biochar-supported metal nanoparticles: A review. *J. Hazard. Mater.* **2020**, *388*, 122026. DOI:10.1016/j.jhazmat.2020.122026
178. Gopalan J, Buthiyappan A, Raman AAA. Insight into metal-impregnated biomass based activated carbon for enhanced carbon dioxide adsorption: A review. *J. Ind. Eng. Chem.* **2022**, *113*, 72–95. DOI:10.1016/j.jiec.2022.06.026
179. Ghosh S, Sarathi R, Ramaprabhu S. Magnesium oxide modified nitrogen-doped porous carbon composite as an efficient candidate for high pressure carbon dioxide capture and methane storage. *J. Colloid Interface Sci.* **2019**, *539*, 245–256. DOI:10.1016/j.jcis.2018.12.063
180. Othman FEC, Yusof N, Samitsu S, Abdullah N, Hamid MF, Nagai K, et al. Activated carbon nanofibers incorporated metal oxides for CO_2 adsorption: Effects of different type of metal oxides. *J. CO_2 Util.* **2021**, *45*, 101434. DOI:10.1016/j.jcou.2021.101434
181. Qamar S, Lei F, Liang L, Gao S, Liu K, Sun Y, et al. Ultrathin TiO_2 flakes optimizing solar light driven CO_2 reduction. *Nano Energy* **2016**, *26*, 692–698. DOI:10.1016/j.nanoen.2016.06.029
182. Khan H, Zavabeti A, Wang Y, Harrison CJ, Carey BJ, Mohiuddin M, et al. Quasi physisorptive two dimensional tungsten oxide nanosheets with extraordinary sensitivity and selectivity to NO_2. *Nanoscale* **2017**, *9*, 19162–19175. DOI:10.1039/c7nr05403c
183. Yang L, Heinlein J, Hua C, Gao R, Hu S, Pfefferle L, et al. Emerging dual-functional 2D transition metal oxides for carbon capture and utilization: A review. *Fuel* **2022**, *324*, 124706. DOI:10.1016/j.fuel.2022.124706
184. Azmi NZM, Buthiyappan A, Patah MFA, Rashidi NA, Raman AAA. Enhancing the CO_2 adsorption with dual functionalized coconut shell-hydrochar using chlorella microalgae and metal oxide: Synthesis, physicochemical properties & mechanism evaluations. *J. Cleaner Prod.* **2024**, *463*, 142736. DOI:10.1016/j.jclepro.2024.142736
185. Ghaemi A, Mashhadimoslem H, Zohourian Izadpanah P. NiO and MgO/activated carbon as an efficient CO_2 adsorbent: characterization, modeling, and optimization. *Int. J. Environ. Sci. Technol.* **2022**, *19*, 727–746. DOI:10.1007/s13762-021-03582-x
186. Nowrouzi M, Younesi H, Bahramifar N. Superior CO_2 capture performance on biomass-derived carbon/metal oxides nanocomposites from Persian ironwood by H_3PO_4 activation. *Fuel* **2018**, *223*, 99–114. DOI:10.1016/j.fuel.2018.03.035
187. Liu W-J, Jiang H, Tian K, Ding Y-W, Yu H-Q. Mesoporous carbon stabilized MgO nanoparticles synthesized by pyrolysis of $MgCl_2$ preloaded waste biomass for highly efficient CO_2 capture. *Environ. Sci. Technol.* **2013**, *47*, 9397–9403. DOI:10.1021/es401286p
188. Gao N, Chen K, Quan C. Development of CaO-based adsorbents loaded on charcoal for CO_2 capture at high temperature. *Fuel* **2020**, *260*, 116411. DOI:10.1016/j.fuel.2019.116411
189. Li Q, Guo J, Xu D, Guo J, Ou X, Hu Y, et al. Electrospun N-doped porous carbon nanofibers incorporated with NiO nanoparticles as free-standing film electrodes for high-performance supercapacitors and CO_2 capture. *Small* **2018**, *14*, 1704203. DOI:10.1002/smll.201704203
190. Xu X, Xu Z, Gao B, Zhao L, Zheng Y, Huang J, et al. New insights into CO_2 sorption on biochar/Fe oxyhydroxide composites: Kinetics, mechanisms, and *in situ* characterization. *Chem. Eng. J.* **2020**, *384*, 123289. DOI:10.1016/j.cej.2019.123289
191. Hosseini S, Bayesti I, Marahel E, Babadi FE, Abdullah LC, Choong TS. Adsorption of carbon dioxide using activated carbon impregnated with Cu promoted by zinc. *J. Taiwan Inst. Chem. Eng.* **2015**, *52*, 109–117. DOI:10.1016/j.jtice.2015.02.015
192. Lahuri AH, Rahim AA, Nordin N, Adnan R, Jaafar NF, Taufiq-Yap YH. Comparative studies on adsorption isotherm and kinetic for CO_2 capture using iron oxide impregnated activated carbon. *Catal. Today* **2023**, *418*, 114111. DOI:10.1016/j.cattod.2023.114111
193. Chen G, Wang F, Wang S, Ji C, Wang W, Dong J, et al. Facile fabrication of copper oxide modified activated carbon composite for efficient CO_2 adsorption. *Korean J. Chem. Eng.* **2021**, *38*, 46–54. DOI:10.1007/s11814-020-0684-1
194. Li M, Huang K, Schott JA, Wu Z, Dai S. Effect of metal oxides modification on CO_2 adsorption performance over mesoporous carbon. *Microporous Mesoporous Mater.* **2017**, *249*, 34–41. DOI:10.1016/j.micromeso.2017.04.033
195. Abdedayem A, Guiza M, Ouederni A. Copper supported on porous activated carbon obtained by wetness impregnation: effect of preparation conditions on the ozonation catalyst's characteristics. *Comptes Rendus Chim.* **2015**, *18*, 100–109. DOI:10.1016/j.crci.2014.07.011

196. Wang X, Cheng H, Ye G, Fan J, Yao F, Wang Y, et al. Key factors and primary modification methods of activated carbon and their application in adsorption of carbon-based gases: A review. *Chemosphere* **2022**, *287*, 131995. DOI:10.1016/j.chemosphere.2021.131995
197. Guo Y, Tan C, Wang P, Sun J, Li W, Zhao C, et al. Magnesium-based basic mixtures derived from earth-abundant natural minerals for CO_2 capture in simulated flue gas. *Fuel* **2019**, *243*, 298–305. DOI:10.1016/j.fuel.2019.01.108
198. Guo Y, Tan C, Sun J, Li W, Zhang J, Zhao C. Biomass ash stabilized MgO adsorbents for CO_2 capture application. *Fuel* **2020**, *259*, 116298. DOI:10.1016/j.fuel.2019.116298
199. Tan B, Cheng G, Zhu X, Yang X. Experimental study on the physisorption characteristics of O_2 in coal powder are effected by coal nanopore structure. *Sci. Rep.* **2020**, *10*, 6946. DOI:10.1038/s41598-020-63988-4
200. Arjona-Jaime P, Morales-Ospino R, Izquierdo MT, Chazaro-Ruiz LF, Celzard A, Rangel-Mendez R, et al. Ca-modified biochar by microwave irradiation for robust CO_2 capture under realistic flue gas conditions. *Chem. Eng. J.* **2025**, *525*, 170349. DOI:10.1016/j.cej.2025.170349
201. Goel C, Mohan S, Dinesha P. CO_2 capture by adsorption on biomass-derived activated char: A review. *Sci. Total Environ.* **2021**, *798*, 149296. DOI:10.1016/j.scitotenv.2021.149296
202. Li H, Zick ME, Trisukhon T, Signorile M, Liu X, Eastmond H, et al. Capturing carbon dioxide from air with charged-sorbents. *Nature* **2024**, *630*, 654–659. DOI:10.1038/s41586-024-07449-2
203. Hsu K-J, Li S, Micari M, Chi H-Y, Villalobos LF, Huang S, et al. Graphene membranes with pyridinic nitrogen at pore edges for high-performance CO_2 capture. *Nat. Energy* **2024**, *9*, 964–974. DOI:10.1038/s41560-024-01556-0
204. Eichler JE, Leonard H, Yang EK, Smith LA, Lauro SN, Burrow JN, et al. Dual-cation activation of N-enriched porous carbons improves control of CO_2 and N_2 adsorption thermodynamics for selective CO_2 capture. *Adv. Funct. Mater.* **2024**, *34*, 2410171. DOI:10.1002/adfm.202410171